telecommunications &
signal processing
laboratory

Ultraspherical Windows: Properties and Computation

Peter Kabal

Department of Electrical & Computer Engineering
McGill University
Montreal, Canada

McGill

Version 1
April 2025

2025/04/07

Revision History:

- 2025-04 v1: Extended material from "Time Windows for Linear Prediction of Speech"

Abstract

This report explores time windows derived from spectra of ultraspherical polynomials. The ultraspherical polynomials use a parameter α, and under particular settings of α, the resulting polynomial becomes either a Chebyshev polynomial of the first kind or second kind, or a Legendre polynomial. These polynomials can be evaluated using a recurrence relationship.

The spectrum of an ultraspherical window is found by evaluating the ultraspherical polynomial at $x = x_0 \cos(\omega/2)$, where x_0 is a second parameter. The resulting spectra have a main lobe (centred at $\omega = 0$) and sidelobes further out. The parameter α determines the behaviour of the sidelobe peaks; larger values of α lead to sidelobe peaks which decay faster with frequency. The parameter x_0 allows for a trade-off between the main lobe width and the peak value of the first sidelobe. The spectra formed from the polynomials correspond to windows that are real and symmetric.

Discrete-time windows can be created by sampling the ultraspherical polynomial spectra and applying an inverse discrete Fourier transform. Alternate means to calculate the windows are described, including procedures that utilize the ultraspherical recurrence relations to directly generate window coefficients. For instance, a window of length N can be formed from windows of length $N-1$ and $N-2$.

With a proper choice of α and x_0, the ultraspherical windows are shown to closely approximate windows created from discrete prolate spheroidal sequences. These DPSS windows minimize the energy in the sidelobes for a given time-bandwidth parameter.

This report also considers continuous-time windows generated as the limit when the number of samples for an ultraspherical window becomes large. These continuous-time windows are directly formulated in the time-domain using a series representation. Sampling these windows can serve as close approximations to discrete-time ultraspherical windows, with their computation being significantly faster than that of the corresponding discrete-time windows.

Highlights

1. Variants of the recurrence formulation for evaluating the ultraspherical polynomial with reduced computational complexity are proposed.
2. The ultraspherical recurrences are applied to directly calculate window coefficients, resulting in fast algorithms that require only basic arithmetic operations.
3. A series computation of sampled continuous-time ultraspherical windows is shown be a computational efficient way to calculate close approximations to discrete-time ultraspherical windows.
4. For sampled continuous-time Dolph-Chebyshev windows, a new approach to choosing the

end-points of the window yields close approximations to discrete-time Dolph-Chebyshev windows.

Ultraspherical Windows

1 Introduction

This report examines properties and computation of time windows with adjustable parameters. These windows have application in a number of areas.

1.1 Window Design of Filters

For the design of filters, in particular lowpass filters, the time response of an ideal lowpass filter (an infinite length sinc function) is time limited by multiplying by a tapered window to mitigate the effect of Gibb's phenomenon [1, §7.5]. The effect of the window in the frequency domain is to convolve the frequency response of the ideal lowpass filter with the frequency response of the window. Design rules allow one to trade off the width of the transition region from passband to stopband against the stopband attenuation.

1.2 Windows for Block Processing of Signals

Another application is the use of time windows to select blocks of samples from an input signal. This selection process allows for analysis of a time localized properties of the input signal. This is the type of processing used in speech and audio coding, and spectral analysis. The frequency response of the windowed signal is the convolution of the spectrum of the input signal with the spectrum of the window.

1.3 Desirable Properties of Windows

Both the time domain and frequency domain properties of the window are important. In the time domain, the window should be non-negative and have a monotonic rise and a monotonic fall. Some windows (for example Dolph-Chebyshev windows) sacrifice monotonicity to achieve a constant peak sidelobe attenuation. These windows have end points which are larger than their neighbours. Some windows can be considered sit on a constant height pedestal. This presence of this pedestal can improve the frequency domain properties. However, from a time domain perspective, the pedestal can cause deleterious effects as shown in [2, §7].

Furthermore it is desirable to have a window which is symmetric about its middle. It is shown in [3] that creating a symmetric window from a nonsymmetric one (by taking the symmetric part) gives a window with a uniformly better frequency response. In some cases, an asymmetric window is used to reduce the look-ahead latency in real time processing [2]. The ultraspherical windows considered here are symmetric.

The frequency response of windows has a main lobe (centred at zero frequency) and sidelobes further out. It is usually desired that the main lobe be compact (as measured, for instance, as the width of the main lobe between zero crossings of the response) and that the sidelobes be attenuated with respect to the main lobe. These are conflicting requirements which involve require a trade-off between main lobe compactness and sidelobe suppression.

The ultraspherical windows described in this report have a parameter α which sets the taper on the sidelobe suppression. Tapered sidelobes mean that the peaks of the sidelobes decrease with distance from the main lobe. A further parameter x_0 sets the trade-off between the main lobe width and the amplitude of the closest-in sidelobe.

A family of windows known as discrete prolate spheroidal sequences (DPSS) minimize the sidelobe energy (not just the peak value of the first sidelobe) for a given main lobe width. There is no closed-form expression for a DPSS, but an ultraspherical window with $\alpha = 1$ provides a good approximation. This report shows that optimizing the value of α can give an even better approximation.

1.4 On-line / Off-line Window Design

The design of ultraspherical discrete-time windows involves an algorithm that for a general window type α requires search for zeros in the frequency response (for setting the main lobe width) or a search for the sidelobe level and the corresponding main lobe level (for setting the sidelobe attenuation). The window can be generated by computing an inverse Discrete Fourier Transform (DFT) of samples of the spectrum. This computation is normally done off-line. If the signal processing application uses only a small number of fixed windows, precomputing them is appropriate.

In some other applications, the windows needed are not known *a priori*. An example is a program that reads a signal file and changes the sampling rate. For example the program in [4] allows for a speech/audio file at one sampling rate to be resampled to a new lower or higher sampling rate. An intermediate step in the sample rate change process requires the filtering of the input data. The filter specifications change depending on the input and output sampling rates. For this application an on-line procedure to design the filter using a windowed ideal lowpass filter is appropriate. The window in question is a sampled continuous-time window, with the window parameters chosen to be appropriate for the sampling rate changes.

2 Ultraspherical Polynomials

The ultraspherical polynomials (also known as Gegenbauer polynomials) are a family of orthogonal polynomials that subsume Chebyshev and Legendre polynomials. They are characterized by a parameter α which determines their behaviour.

The ultraspherical polynomials, $C_m^{(\alpha)}(x)$, satisfy the following recurrence relation,

$$\begin{aligned} C_m^{(\alpha)}(x) &= \left(2+2\frac{\alpha-1}{m}\right)xC_{m-1}^{(\alpha)}(x) - \left(1+2\frac{\alpha-1}{m}\right)C_{m-2}^{(\alpha)}(x), \\ & m \geq 2;\ C_0^{(\alpha)}(x) = 1, C_1^{(\alpha)}(x) = 2\alpha x. \end{aligned} \tag{1}$$

$C_m^{(\alpha)}(x)$ is a polynomial of order m in x. From the recurrence equation, it can be seen that $C_m^{(\alpha)}(x)$ contains only odd (resp. even) powers of x when m is odd (resp. even). As a consequence $C_m^{(\alpha)}(x)$ is an odd or even function of x depending on the value m. The recurrence in m allows for a generic computation of the polynomial for a given value of x. In the special cases noted below, closed-form expressions in terms of elementary transcendental functions are available.

Ultraspherical polynomials $C_m^{(\alpha)}(x)$ and $C_n^{(\alpha)}(x)$ are orthogonal over the interval $[-1,+1]$ with respect to the weighting function $(1-x^2)^{\alpha-1/2}$ when $m \neq n$, $\alpha > -1/2$, and $\alpha \neq 0$ [5]. The zero crossings and finite extrema occur in the $[-1,+1]$ interval. Outside the interval, the value shoots off to $\pm\infty$. Figure 1 shows an example of an ultraspherical polynomial for $M = 19$. Since M is odd, the polynomial is an odd function of x.

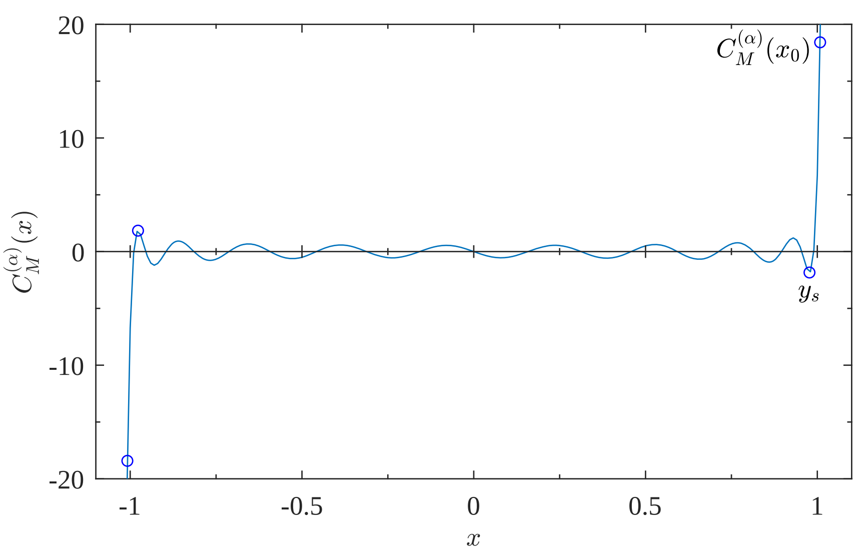

Fig. 1 A plot of $C_M^{(\alpha)}(x)$ for $M = 19$ and $\alpha = 0.8$ against x. The point $x = x_0$ gives a value $C_M^{(\alpha)}(x_0) = 10|y_s|$.

2.1 Special Cases

The ultraspherical polynomials are a special case of the hypergeometric polynomials. The ultraspherical polynomials become well-known polynomials for specific values of α.

Chebyshev polynomial of the first kind, $\alpha = 0$

For $\alpha = 0$, with an appropriate limiting operation, the ultraspherical polynomial becomes a Chebyshev polynomial of the first kind [5],

$$T_m(x) = \frac{m}{2} \lim_{\alpha \to 0} \frac{C_m^{(\alpha)}(x)}{\alpha}, \tag{2}$$

$$T_m(x) = 2xT_{m-1}(x) - T_{m-2}(x), \qquad m \geq 2;\ T_0(x) = 1, T_1(x) = x. \tag{3}$$

The Chebyshev polynomial $T_m(x)$ can be written as [6, §1.4]

$$T_m(x) = \begin{cases} (-1)^m \cosh\bigl(m \cosh^{-1}(-x)\bigr), & x \leq -1, \\ \cos\bigl(m \cos^{-1}(x)\bigr), & -1 \leq x \leq +1, \\ \cosh\bigl(m \cosh^{-1}(x)\bigr), & x \geq +1. \end{cases} \tag{4}$$

Legendre polynomial, $\alpha = 1/2$

The Legendre polynomials result when $\alpha = \frac{1}{2}$,

$$P_m(x) = C_m^{(1/2)}(x), \tag{5}$$

$$P_m(x) = \frac{1}{m}\bigl(x(2m-1)P_{m-1}(x) - (m-1)P_{m-2}(x)\bigr), \qquad m \geq 2;\ P_0(x) = 1, P_1(x) = x. \tag{6}$$

Chebyshev polynomial of the second kind, $\alpha = 1$

Chebyshev polynomials of the second kind result when $\alpha = 1$.

$$U_m(x) = C_m^{(1)}(x), \tag{7}$$

$$U_m(x) = 2xU_{m-1}(x) - U_{m-2}(x), \qquad m \geq 2;\ U_0(x) = 1, U_1(x) = 2x. \tag{8}$$

The recurrence relation for $\alpha = 1$ is the same as for $\alpha = 0$, only the initial conditions differ. The Chebyshev polynomial $U_m(x)$ can be written as [6, §1.4]

$$U_m(x) = \begin{cases} (-1)^m \dfrac{\sinh\big((m+1)\cosh^{-1}(-x)\big)}{\sinh\big(\cosh^{-1}(-x)\big)}, & x < -1, \\ (-1)^m (m+1), & x = -1, \\ \dfrac{\sin\big((m+1)\cos^{-1}(x)\big)}{\sin\big(\cos^{-1}(x)\big)}, & -1 < x < +1, \\ m+1, & x = +1, \\ \dfrac{\sinh\big((m+1)\cosh^{-1}(x)\big)}{\sinh\big(\cosh^{-1}(x)\big)}, & +1 < x. \end{cases} \tag{9}$$

3 Discrete-Time Ultraspherical Windows

Streit [5] introduced the use of the ultraspherical family of polynomials for window design. The idea was picked up by Deczky [7], and Bergen and Antoniou [8].

The parameter α will set the type of window, with discrete values giving some well-known window types. For $\alpha = 0$, one gets Dolph-Chebyshev windows (based on Chebyshev polynomials of the first kind); for $\alpha = 1$, one gets Saramäki windows (based on Chebyshev polynomials of the second kind) [9]. The parameter α controls how fast the sidelobe amplitudes fall off. For α negative, the sidelobe amplitudes increase with frequency. For such a setting, the window coefficients can become negative — normally not an appropriate property for a window.

3.1 Frequency Response

An ultraspherical polynomial of order M will be used to form the frequency response corresponding to a $N = M + 1$ coefficient symmetrical window. Consider the substitution, $x = x_0 \cos(\omega/2)$. This maps the ω-interval $[0, 2\pi]$ to the x-interval $[-x_0, +x_0]$ in reverse. This transformation has the effect of warping the x axis. The values of the maxima and minima of the polynomial within the interval are unchanged by this transformation.

Define

$$B_m^{(\alpha)}(\omega) = C_m^{(\alpha)}(x_0 \cos(\omega/2)). \tag{10}$$

This composite function is a periodic zero-phase response.[1]

For m even (resp. odd), $C_m^{(\alpha)}(x)$ is an even (resp. odd) function about $x = 0$.

$$C_m^{(\alpha)}(x) = \begin{cases} C_m^{(\alpha)}(-x), & m \text{ even}, \\ -C_m^{(\alpha)}(-x), & m \text{ odd}. \end{cases} \tag{11}$$

Using the symmetry/anti-symmetry of $C_m^{(\alpha)}(x)$, gives

$$B_m^{(\alpha)}(\omega + 2\pi k) = \begin{cases} B_m^{(\alpha)}(\omega), & m \text{ even or } k \text{ even}, \\ -B_m^{(\alpha)}(\omega), & m \text{ odd and } k \text{ odd}. \end{cases} \tag{12}$$

For m even, the period of $B_m^{(\alpha)}(\omega)$ is 2π and the spectrum is symmetric with respect to $\omega = \pi$. For m odd, the period is 4π and the spectrum is anti-symmetric with respect to $\omega = \pi$. Given the parity of m, $B_m^{(\alpha)}(\omega)$ is completely determined by its values for $0 \le \omega \le \pi$.

[1] A zero-phase response is a real, even function of ω. The zero-phase property is a bit of a misnomer since the response can take on positive and negative values.

Figure 2 shows a plot of the frequency response $B_M^{(\alpha)}(\omega)$ corresponding to the ultraspherical polynomial $C_M^{(\alpha)}(x)$ shown in Fig. 1.

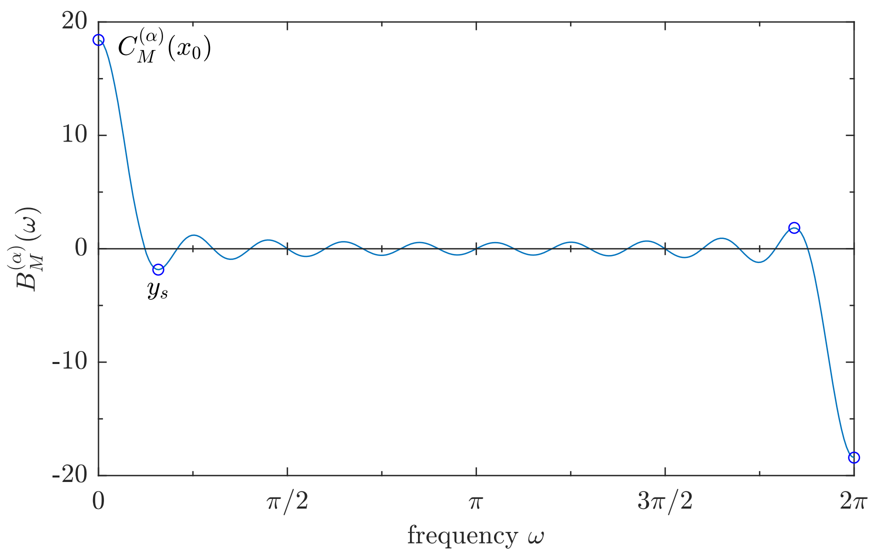

Fig. 2 A plot of $B_M^{(\alpha)}(\omega)$ for $M = 19$, $\alpha = 0.8$ and a main lobe to sidelobe ratio of 10.

Spectrum for a Dolph-Chebyshev window, $\alpha = 0$

Setting $x = x_0 \cos(\omega/2)$ in Eq. (4), the zero-phase frequency response for $\alpha = 0$ is

$$B_{N-1}^{(0)}(\omega) = T_{N-1}(x_0 \cos(\omega/2)), \tag{13}$$

where $T_m(x)$ is given by Eq. (4).

Spectrum for a Saramäki window, $\alpha = 1$

Setting $x = x_0 \cos(\omega/2)$ in Eq. (9), the zero-phase frequency response for $\alpha = 1$ is

$$B_{N-1}^{(1)}(\omega) = U_{N-1}(x_0 \cos(\omega/2)), \tag{14}$$

where $U_m(x)$ is given by Eq. (9).

3.2 Window Derivation from the Frequency Response

For a polynomial of order $N-1$ (N coefficients), form

$$W(\omega) = e^{-j\omega(N-1)/2} B_{N-1}^{(\alpha)}(\omega). \tag{15}$$

This operation converts the zero-phase response $B_{N-1}^{(\alpha)}(\omega)$ to a linear phase response $W(\omega)$. The response $W(\omega)$is periodic with period 2π for both N odd and N even. It is the Discrete-Time Fourier Transform (DTFT) of an N term discrete-time window sequence $w[n]$,

$$W(\omega) = \sum_{n=0}^{N-1} w[n] e^{-j\omega n}. \tag{16}$$

The window coefficients can be found as the inverse Discrete Fourier Transform of samples of the frequency response $W(\omega)$.

3.2.1 Derivation for N odd

For N odd, the steps in deriving the DTFT of the window coefficients Eq. (16) are as follows.

$$\begin{aligned}
W(\omega) &= e^{-j\omega\frac{N-1}{2}} B_{N-1}^{(\alpha)}(\omega) \\
&= e^{-j\omega\frac{N-1}{2}} C_{N-1}^{(\alpha)}(x_0\cos(\omega/2)) \\
&= e^{-j\omega\frac{N-1}{2}} \sum_{k=0}^{(N-1)/2} a_{2k}\big(x_0\cos(\omega/2)\big)^{2k} && \text{(a)} \\
&= e^{-j\omega\frac{N-1}{2}} \sum_{n=0}^{(N-1)/2} b_n \cos(\omega n) && \text{(b)} \\
&= \frac{1}{2} e^{-j\omega\frac{N-1}{2}} \sum_{n=0}^{(N-1)/2} b_n \big(e^{j\omega n} + e^{-j\omega n}\big) && \text{(c)} \\
&= \sum_{n=0}^{(N-1)/2} c_n e^{-j\omega n} + \sum_{n=(N-1)/2}^{N-1} c_n e^{-j\omega n} \\
&= \sum_{n=0}^{N-1} w[n] e^{-j\omega n}. && \text{(d)}
\end{aligned} \tag{17}$$

(a) For N odd, $C_{N-1}^{(\alpha)}(x)$ is a polynomial in even powers of x. The coefficients a_{2k} can be calculated using the recurrence relation in Eq. (1). The coefficients will be augmented to absorb the term x_0^{2k}.

(b) A power series with terms $a_k x^k$ can be expressed as an expansion in Chebyshev polynomials of the first kind with terms $b_n T_n(x)$. A recurrence relation can be used to calculate the coefficients b_n from the coefficients a_k [10, §28.3]. The power series has only terms with even powers of x resulting in an expansion with only even order Chebyshev polynomial terms [11, §3.2]. When $x = \cos(\phi)$, $T_n(x) = \cos(\phi n)$. With $\phi = \omega/2$, the result is an expansion with $\cos(\omega n)$ terms.

(c) Expanding the cosine as complex exponentials, the linear phase component can be brought inside the summations. The coefficient $c_n = b_{|n-(N-1)/2|}/2$.

(d) Noting that the term $c_{(N-1)/2}$ appears in both summations, then $w[n] = c_n$ for $n \neq (N-1)/2$ and $w[(N-1)/2] = 2\,c_{(N-1)/2}$. The window is symmetric with $w[n] = w[N-1-n]$. The window has a Type I linear phase frequency response [12].

The N-point window $w[n]$ can be computed as the inverse DFT of samples of the spectrum evaluated at $\omega_k = 2\pi k/N$,

$$w[n] = \frac{1}{N} \sum_{k=0}^{N-1} W(\omega_k) e^{j\omega_k n}, \tag{18}$$

where $W(\omega) = e^{-j\omega \frac{N-1}{2}} B_{N-1}^{(\alpha)}(\omega)$. Noting the symmetry in the spectrum, for N odd the inverse DFT can be written using only real computations as

$$w[n] = \frac{1}{N} \Big[B[0] + 2 \sum_{k=1}^{(N-1)/2} B[k] \cos\Big(\frac{2\pi k}{N} \big(n - \frac{N-1}{2} \big) \Big) \Big], \tag{19}$$

where $B[k] = B_{N-1}^{(\alpha)}(\omega_k)$, with $B[k] = B[N-k]$. This equation can be evaluated for $n = 0, \ldots, (N-1)/2$ and the remaining values determined from the symmetry of $w[n]$.

3.2.2 Derivation for N even

For N even, the development deviates from the case for N odd at the third line in Eq. (17).

$$
\begin{aligned}
W(\omega) &= e^{-j\omega\frac{N-1}{2}} \sum_{k=0}^{N/2-1} a_{2k+1} (x_0 \cos(\omega/2))^{2k+1} && \text{(a)} \\
&= e^{-j\omega\frac{N-1}{2}} x_0 \cos(\omega/2) \sum_{n=0}^{N/2-1} b_n \cos(\omega n) && \text{(b)} \\
&= e^{-j\omega\frac{N-1}{2}} \frac{x_0}{2} \bigl(e^{j\omega/2} + e^{-j\omega/2}\bigr) \frac{1}{2} \sum_{n=0}^{N/2-1} b_n \bigl(e^{j\omega n} + e^{-j\omega n}\bigr) \\
&= \frac{x_0}{2} (1 + e^{-j\omega}) e^{-j\omega N/2} \frac{1}{2} \Bigl[\sum_{n=-(N/2-1)}^{0} b_{-n} e^{-j\omega n} + \sum_{n=0}^{N/2-1} b_n e^{-j\omega n} \Bigr] && \text{(c)} \\
&= \frac{x_0}{2} (1 + e^{-j\omega}) \sum_{n=0}^{N-2} c[n] e^{-j\omega n} && \text{(d)} \\
&= \sum_{n=0}^{N-1} w[n] e^{-j\omega n}. && \text{(e)}
\end{aligned}
\tag{20}
$$

(a) For N even, $C_{N-1}^{(\alpha)}(x)$ is a polynomial with odd powers of x.

(b) After factoring out $x_0 \cos(\omega/2)$, the sum is back to the same form as for an odd number of coefficients and can be expressed as a Chebyshev expansion. The $\cos(\omega/2)$ term outside the sum shows that the frequency response has a null at $\omega = \pi$.

(c) Each cosine term is expressed as a complex exponential. The sum terms are rewritten to have the same exponent. Note that the term b_0 appears in both summations.

(d) The two sums have been combined to create an $N-1$ term symmetric sequence. The coefficient $c[n] = 0.5\, b_{|n-(N/2-1)|}$ for $n \neq N/2-1$ and $c[N/2+1] = b_0$. The $N-1$ coefficients are symmetric, $c[n] = c[N-2-n]$

(e) The last step is to incorporate the multiplicative two term frequency response which appears outside the sum. The product of frequency responses corresponds to convolution of a two term time response with the coefficients $c[n]$. The convolution gives $w[n] = (x_0/2)\bigl(c[n] + c[n-1]\bigr)$. The final window has an even number of terms and is symmetric with $w[n] = w[N-1-n]$. The window has a Type II linear phase frequency response [12].

The general formulation in Eq. (18) with $\omega_k = 2\pi k/N$, can be used for N even. Noting the symmetry of the spectrum, for N even, the inverse DFT can also be written as

$$
w[n] = \frac{1}{N} \Bigl[B[0] + 2 \sum_{k=1}^{N/2-1} B[k] \cos\Bigl(\frac{2\pi k}{N} \bigl(n - \frac{N-1}{2}\bigr) \Bigr) \Bigr], \tag{21}
$$

where $B[k] = B^{(\alpha)}_{N-1}(\omega_k)$, with $B[k] = -B[N-k]$ (implies that $B[N/2] = 0$).

3.2.3 Alternate formulation for N even

An alternate formulation can be used to find $w[n]$ for even N. This is suggested by the steps in Eq. (20). At Step (b), the term $x_0 \cos(\omega/2)$ appears outside the sum. Let the sum be designated as

$$B^{\dagger}(\omega) = B^{(\alpha)}_{N-1}(\omega) / \big(x_0 \cos(\omega/2)\big). \tag{22}$$

This real response satisfies $B^{\dagger}(\omega) = -B^{\dagger}(2\pi - \omega)$. Then at Step (d)

$$e^{-j\omega N/2} B^{\dagger}(\omega) = \sum_{n=0}^{N-2} c[n] e^{-j\omega n}, \tag{23}$$

where $c[n]$ is an odd length symmetric sequence. The coefficients $c[n]$ can be found as the inverse DFT of samples of $e^{-j\omega N/2} B^{\dagger}(\omega)$. Define $M = N - 1$. Sample $e^{-j\omega(M-1)/2} B^{\dagger}(\omega)$ at M values $\omega'_k = 2\pi/M$. The inverse DFT of these M samples gives $c[n]$. This transform can be calculated using Eq. (19) with N replaced by M and $B[k]$ replaced by $B^{\dagger}[k]$, where the $B^{\dagger}[k]$ are samples of $B^{\dagger}(\omega)$.

Finally, defining $c[n]$ to be zero outside the interval $0 \leq N-2$, the window coefficients are given by smoothing $c[n]$ to give $w[n] = x_0\big(c[n] + c[n-1]\big)/2$ for $0 \leq n \leq N-1$. This last step compensates for the earlier division by $x_0 \cos(\omega/2)$.

A modification to the ultraspherical polynomial recurrence avoids the need to divide the spectrum by $x_0 \cos(\omega/2)$. The scheme is outlined in Appendix A. Setting $x = x_0 \cos(\omega/2)$, the modified recurrence directly computes the values of $B^{\dagger}(\omega)$. After computing the coefficients $c[n]$, smoothing is used to give the window values.

3.3 Design of Ultraspherical Windows

The ultraspherical windows have three parameters N, x_0, and α. Consider the case of a fixed N and α. The parameter x_0 orchestrates the trade-off between sidelobe suppression and main lobe width. As such, ultraspherical windows can be designed by specifying the desired sidelobe attenuation, or by specifying the desired main lobe width.

For $N = 1$, the window consists of one point and the corresponding spectrum is constant. There are no sidelobes. For $N = 2$, the window consists of two equal values. There is null in the spectrum at $\omega = \pi$. The spectrum is all main lobe; there is no sidelobe.

3.3.1 Sidelobe attenuation

For $N > 2$, an estimate of the height of the first sidelobe is obtained by examining the sidelobe between appropriate zero crossings. The zero crossings can be numbered with k, where $k = 1$ gives the largest zero crossing (just below $x = 1$), $k = 2$, gives the second largest zero crossing, and so on. An estimate of the position of the kth zero crossing is given by

$$\tilde{x}_k = \frac{x_k^{(0)} x_k^{(1)}}{\alpha x_k^{(1)} + (1-\alpha) x_k^{(0)}}, \tag{24}$$

where $x_k^{(0)}$ is the kth zero crossing of the Chebyshev polynomial of the first kind ($\alpha = 0$), and $x_k^{(1)}$ is the kth zero crossing of the Chebyshev polynomial of the second kind ($\alpha = 1$). The zero crossings $x_k^{(0)}$ are determined from the middle line of Eq. (4) and the $x_k^{(1)}$ are determined from the middle line of Eq. (9),

$$x_k^{(0)} = \cos\left(\frac{\pi}{2}\frac{2k-1}{N-1}\right), \qquad x_k^{(1)} = \cos\left(\pi\frac{k}{N}\right), \qquad 1 \le k \le N-1. \tag{25}$$

The estimate in Eq. (24) is based on a linear combination of the inverses of the known roots. The estimate can be used both for α inside of the interval $[0, 1]$ and for reasonable values of α outside of that interval.

The sidelobe attenuation will be measured by the factor R, where R is the ratio of the height of the main lobe to the height of the first sidelobe. Measured in dB, it is the attenuation of the sidelobe. To find the sidelobe amplitude, first estimate the position of the second to last zero crossing $\tilde{x}_2$. Search for the largest sidelobe amplitude in the interval $[\tilde{x}_2, 1]$. Let the largest sidelobe amplitude be denoted as y_s. Then, given a desired main lobe to sidelobe ratio R, search for the value x_0 which sets $C_M^{(\alpha)}(x_0) = R\,|y_s|$. The plot in Fig. 1 shows the ultraspherical polynomial for $M = 19$, $\alpha = 0.8$, and $R = 10$, giving $x_0 = 1.008$. The positions of the peak of the first sidelobe y_s, and $C_M^{(\alpha)}(x_0)$ are marked with circles on this plot.

3.3.2 Main lobe width

An alternative design criterion is to set the width of the main lobe of the frequency response to a given value. For $N > 1$, the main lobe width is the distance in the (periodic) frequency response between the first zero crossings around the peak response at $\omega = 0$. Let the first positive zero be at location ω_z. The main lobe width in radian frequency is $2\omega_z$, or ω_z/π in natural frequency (Hz).

The mapping from ω to x is $x = x_0 \cos(\omega/2)$. The point ω_z corresponds to x_1 where x_1 is the largest zero in the ultraspherical polynomial $C_{N-1}^{(\alpha)}(x)$. For a general α, a search for x_1 is conducted in the interval $[(\tilde{x}_2 + \tilde{x}_1)/2, 1]$.[2]

It is useful to create a dimensionless parameter to describe the main lobe width. The parameter σ is defined to be the ratio of the main lobe width of a window to the main lobe width for a rectangular window,

$$\sigma = \frac{\omega_z}{2\pi/N} = \frac{N}{\pi}\cos^{-1}\left(\frac{x_1}{x_0}\right). \tag{26}$$

The largest value of ω_z is π (when $x_1 = 0$), giving $\sigma \le N/2$.

Dolph-Chebyshev window, $\alpha = 0$

The ultraspherical window with $\alpha = 0$ is the Dolph-Chebyshev window [13]. This window has the narrowest main lobe (measured between zero crossings) for a given side lobe attenuation. The Dolph-Chebyshev window has equiripple side lobes.

For $\alpha = 0$, the Chebyshev polynomial of the first kind has the explicit formula given in Eq. (4). The extrema in the interval $[-1, +1]$ have a magnitude of 1. For $N \ge 2$, the value of x_0 is found by solving $T_{N-1}(x_0) = R$ for x_0, giving

$$x_0 = \cosh\Big(\frac{\cosh^{-1}(R)}{N-1}\Big). \tag{27}$$

Inverting this equation, R is found from x_0 as

$$R = \cosh\big((N-1)\cosh^{-1}(x_0)\big). \tag{28}$$

The Dolph-Chebyshev window can also be designed to give a specific value of σ to set the main lobe width. The zero crossing parameter x_1 for $\alpha = 0$ is given in Eq. (25). Then solving Eq. (26) for x_0 gives

$$x_0 = \frac{x_1}{\cos(\sigma\frac{\pi}{N})}, \qquad \text{where } x_1 = \cos\left(\frac{\pi}{2(N-1)}\right). \tag{29}$$

As a lower extreme, set $R = 1$ giving $x_0 = 1$. Equation (25) gives x_1. Then from Eq. (26), the main lobe width parameter is $\sigma = {}^1\!/\!_2\, N/(N-1)$. For $x_0 = 1$, the spectrum is a sinusoid with period $4\pi/(N-1)$ corresponding to $(N-1)/2$ periods in the interval $[0, 2\pi]$. The window itself is zero except for the end samples.

As R increases, x_0 increases, and the middle of the windows starts to fill in. From Eq. (26), σ also increases. Later, Fig. 8 shows the window for $N = 240$ and $\sigma = 1$. In the limit of large R and large x_0, the unnormalized window coefficients are given by a binomial distribution [14],

$$\omega[n] = \binom{N-1}{n}, \qquad 0 \le n \le N-1. \tag{30}$$

[2]For $\alpha < 0$, the zero may occur above 1.

Let the ultraspherical window for a given R be $w[n]$. The middle points give a bell-shaped response with a monotonic rise and a monotonic fall. The end coefficients of $w[n]$ are larger than the adjacent coefficients. Let $w[n]$ be decomposed as the sum of $w_{sx}[n]$ (the bell-shaped response) and $w_{px}[n]$ which adds a pulse to each end coefficient. The internal samples of $w_{sx}[n]$, $1 \leq n \leq N-2$, are equal to the corresponding coefficients in $w[n]$. The end points of $w_{sx}[n]$ and the end points of $w_{px}[n]$ add to form the end points of $w[n]$.

Let the corresponding zero-phase responses be $B(\omega)$, $B_{sx}(\omega)$, and $B_{px}(\omega)$. Note that the frequency response at $\omega = 0$ is the sum of the corresponding time samples. Let $B_{px}(0) = B(0)/R$. This defines the non-zero samples of $w_{px}[n]$ as

$$w_{px}[n] = w_{px}[N-1] = \frac{1}{2R} \sum_{n=0}^{N-1} w[n]. \tag{31}$$

Noting that $w[0] = w[N-1]$, the end points of $w_{sx}[n]$ are

$$w_{sx}[0] = w_{sx}[N-1] = w[0] - w_{px}[0]. \tag{32}$$

Using this decomposition of $w[n]$, the sum of the constant amplitude sinusoidal frequency response adds to the decaying frequency response of the bell-shaped part of the window to give the equiripple response for a Dolph-Chebyshev window.[3] Figure 3 shows the two components of the frequency response adding together to give an equiripple response. The Dolph-Chebyshev window ($N = 240$) was designed with a sidelobe attenuation factor of $R = 10$ (20 dB), giving $\sigma = 1.080$.

Appendix D further explores the decomposition of $w[n]$ leading to $w_{sx}[n]$ and $w_{px}[n]$. It is shown that knowledge of $w[n]$ for $1 \leq n \leq N-1$ and R can be used to find $w[0]$, $w_{sx}[0]$, and $w_{px}[0]$.

Saramäki window, $\alpha = 1$

For $\alpha = 1$, the ultraspherical window is the Saramäki window [9].[4] This window approximates a discrete prolate spheroidal sequence (DPSS). A DPSS minimizes the energy of the sidelobes.

The design of a Saramäki window with the main lobe parameter σ is straightforward. The

[3]This approach is motivated by a similar decomposition of the continuous-time Dolph-Chebyshev window – see the discussion leading to Fig. 8.

[4]See §B.3 for comments on the method used to calculate the windows in [9].

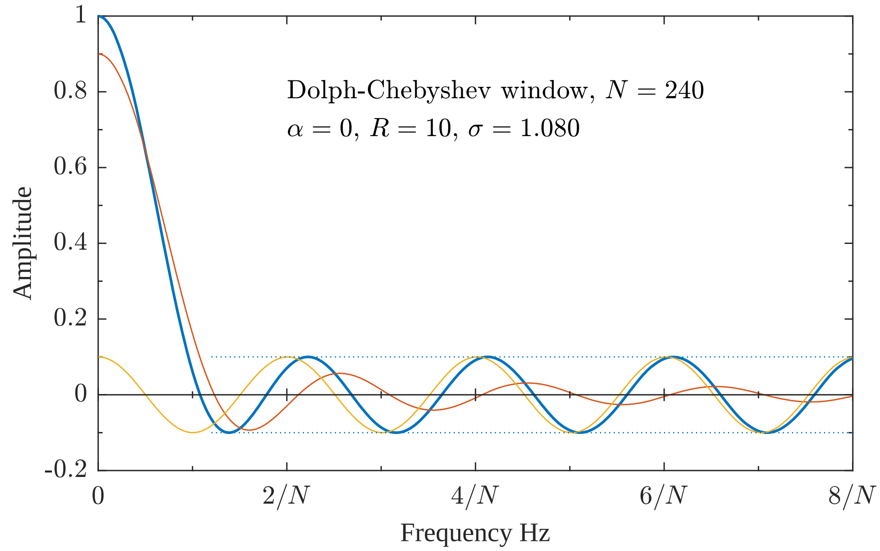

Fig. 3 Zero-phase frequency response of a Dolph-Chebyshev window with $N = 240$ and $R = 10$. The thick line is the equiripple frequency response $B(\omega)$. It is the sum of the response with decaying sidelobes $B_{sx}(\omega)$ and the constant amplitude sinusoidal response $B_{px}(\omega)$.

value of x_1 is known from Eq. (25). Solving Eq. (26) for x_0 gives

$$x_0 = \frac{x_1}{\cos(\sigma\frac{\pi}{N})}, \qquad \text{where } x_1 = \cos(\frac{\pi}{N}). \tag{33}$$

A general procedure to get a window with a given value of R is more complicated. First, a search for the sidelobe level is carried out. Then a search for the point on the response which is R times larger determines x_0.

For a Saramäki window, the stopband response is given by the middle part of Eq. (9). This response is of the form of a digital sinc function, $\sin(N\theta/2)/\sin(\theta/2)$. The sidelobe peaks occur when the slope of this response is zero. Setting the slope to zero gives the transcendental equation [6, §2.2],

$$\tan(N\theta_s/2) = N\tan(\theta_s/2) \neq 0. \tag{34}$$

The first sidelobe is in the interval $2\pi/N < \theta_s < 3\pi/N$, close to the top end of this range. The peak value is

$$y_s = \frac{\sin(N\theta_s/2)}{\sin(\theta_s/2)}. \tag{35}$$

The Saramäki window becomes a rectangular window when $\sigma = 1$ giving $x_0 = 1$. With those parameters, the frequency response is $\sin(N\omega/2)/\sin(w/2)$ for all ω. The value of R for the rectangular window depends on N, but asymptotically for large N it reaches the value $R = 4.56$ (13.26 dB). This value will appear again in the discussion of Eq. (61).

For $\sigma < 1$, the window becomes bowl shaped – the ends are pinned to the values for the rectangular window corresponding to $\sigma = 1$, while the middle samples sag downward. For $\sigma \lessapprox 0.646$ ($R \lessapprox 1.3$), the middle part of the window goes negative.

3.4 Window Normalization

Odd length windows are typically normalized by setting the middle coefficient to one. However, for ultraspherical windows, for instance when $\alpha = 0$, the middle coefficient may not be the largest. In some case, the end coefficients are larger than the middle coefficient.

For N even, there is no single middle coefficient. While interpolating between the two middle coefficients often yields a value that could serve as a normalization factor, there does not seem to be an interpolation method that is completely compatible with the polynomial/periodic nature of the window spectrum.[5]

As an expedient to handle both the case where coefficients in the middle are smaller than the end coefficients[6] and the case of N even, the coefficients can be normalized by the value of the coefficient with the largest magnitude,

$$\widetilde{w}[n] = \frac{w[n]}{w[k]}, \qquad \text{where } k = \arg\max_{n} |w[n]|. \tag{36}$$

The normalized value of that coefficient will be +1. For $\alpha \geq 1$, the window will have middle coefficient set to 1 for N odd, and the middle two coefficients set to 1 for N even. For $0 \leq \alpha < 1$, the largest coefficients may be the end coefficients.

Nonetheless there are situations when it is desired to normalize even length windows in such a way as to be able to fairly compare them with odd length windows. In that case, a cubic spline interpolation can be used to *estimate* the height of an even length window at the mid-point (between samples) of the window. A spline based on 3 samples to either side of the mid-point is suggested. This procedure was tested on sampled continuous-time windows for which the true value of the mid-point is known. Windows with lengths of 24, 120, and 240 were created for a Hann window, and the continuous-time ultraspherical windows that are introduced in §4. For $N = 24$, the normalized window coefficients using the true value of the mid-point and those using the estimated

[5] At first, normalizing the odd length sequence $c[n]$ appears in Step (d) of Eq. (20) looked promising. However, further analysis showed that the envelope of $c[n]$ has a saw-tooth pattern, resulting in a middle coefficient unsuitable for normalization.

[6] In the extreme case of $\alpha = 0$ with $R = 1$, the middle coefficients are theoretically zero, and computationally can even be slightly negative.

value, agree to around 6 digits. For $N = 120$, the estimated result was correct to 8–9 digits, and for $N = 240$, to 9–11 digits. It is interesting to note that increasing the number of knots in the spline formulation beyond 6 did not significantly improve the mid-point estimation, and in some cases actually made the estimate marginally less accurate.

3.5 Computational considerations

Different approaches to calculating ultraspherical windows were implemented in MATLAB using double-precision floating-point arithmetic. The routines employ vector operations when convenient.

3.5.1 Inverse DFT approach

The inverse DFT (IDFT) approach first computes spectral samples using the modified ultraspherical polynomial recurrence relation in §A.2. The accuracy of the spectral samples was validated for the case of $\alpha = 0$ and $\alpha = 1$ for which explicit formulas are available, i.e., Eq. (4) and Eq. (9). For $N = 1024$, the spectra (normalized to unity at $\omega = 0$) have a maximum absolute difference of the order 10^{-12} between the polynomial recurrence calculation and the explicit formulas.[7]

The window is calculated using an inverse DFT, with the realness of the spectral samples and the realness of the window coefficients, along with their symmetry, are used to reduce the computational load. For N odd/even, the real computations according to Eq. (19)/Eq. (21) are used.

3.5.2 Recurrence formulation

Appendix B describes several approaches to calculating the window coefficients using the ultraspherical recurrence relationship. These procedures avoid the evaluation of trigonometric functions. The first uses the basic ultraspherical recurrence. The window coefficients for order m are determined from the coefficients for windows of order $m-1$ and $m-2$. The second procedure using the modified recurrence equations described in §A.2. This algorithm uses alternating recurrence relationships for m even and m odd. These window recurrence relationships do not seem to have been previously described.

---

[7]Samples of the spectrum were also calculated by first determining the direct-form polynomial coefficients using the algorithm of §A.2.1. Due to the huge dynamic range of the polynomial coefficients, the evaluation of the spectral samples was only useful for small values of N. For $N = 256$, the loss of precision in adding large positive and large negative values gave bogus results, and for $N = 1024$, calculating of the coefficients themselves resulted in positive and negative overflows.

A third procedure uses a double-step recurrence relationship to compute a window of length N in terms of the windows of length $N-2$ and $N-4$. This is a reinterpretation of the double-step calculation described in Rowińska-Schwarzweller and Wintermantel [15].

The basic recurrence relation is the simplest to program. The modified recurrence procedure treats even/odd order steps differently to achieve a reduction in average computational complexity. The double-step procedure is more complicated at each (double) step, but requires half as many steps.

Routines to calculate ultraspherical windows were implemented based on the recurrences on the coefficient vectors. Table 1 shows the relative average times for calculating the different window recurrences.[8] The double-step procedure is the fastest;[9] the modified recurrence formulations takes about 5% more time, and the basic recurrence formulation takes about 50% more time. The modified recurrence procedure is a good compromise between program simplicity and computational speed.

Table 1 Relative Window Calculation Times, $R = 60$ dB, $\alpha = 1$

Window Calculation	$N = 240$ Time	$N = 1024$ Time
Basic Recurrence	1.48	6.75
Modified Recurrence	1.03	4.95
Twp-Step Recurrence	1.00	4.69

3.5.3 Power series calculation

A direct formula for the window coefficients using a power series calculation is available [5, 7, 8].[10] For $x_0 > 1$,

$$w[n] = \frac{A}{M-n} \binom{\alpha + M - n - 1}{M - n - 1} \sum_{m=0}^{n} \binom{\alpha + n - 1}{n - m} \binom{M - n}{m} D_0^m, \qquad 0 \le n \le \lfloor N/2 \rfloor, \tag{37}$$

[8]For each candidate method, he measurement used a single invocation as warmup and then measured the time to run the candidate 1000 times.

[9]On a PC (vintage 2021), for $N = 240$ the average computation time for the double-step recurrence formulation is about 0.31 ms.

[10]Some references indicate incorrectly that the equation can give the coefficients for $0 \le n \le N-1$.

where $M = N - 1$, $w[M - n] = w[n]$, $D_0 = 1 - x_0^{-2}$, and

$$A = \begin{cases} \alpha x_0^M, & \alpha \neq 0, \\ x_0^M, & \alpha = 0. \end{cases} \tag{38}$$

The generalized binomial coefficient with integer or non-integer value a can be calculated with the recursion,

$$\binom{a}{k} = \frac{a - k + 1}{k} \binom{a}{k-1}, \qquad \text{while } k \geq 1, \text{ with } \binom{a}{0} = 1. \tag{39}$$

In the power series formula, the term D_0 is positive and less than one when $x_0 > 1$. The binomial coefficient terms in the summation can become huge, but when multiplied by D_0^m, the result is reined in. Underflows of the D_0^m terms occur for modest values of m. An underflow sets the computed value of D_0^m to zero. When m is large enough to invoke underflows, the corresponding zero-valued terms in the summation can be omitted. For instance with $N = 1024$, terms for which m is larger than about 75 (depends on α) need not be computed.

For a sufficiently large N, there is a problem in computing the generalized binary coefficient that appears outside the summation. The recursive computation of this term can return spurious values. The following computation can be used instead[11]

$$\binom{a}{k} = \exp\bigl(\log\Gamma(a+1) - \log\Gamma(k+1) - \log\Gamma(a-k+1)\bigr). \tag{40}$$

3.5.4 Comparison of window computation approaches

Three contenders for methods to compute the ultraspherical window coefficients will be compared: the inverse DFT (IDFT) approach, the modified window recurrence of §B.2, and the power series calculation. The tests were conducted with small (23, 24), medium (239, 240), and large (1023, 1024) values for N,[12] a sidelobe attenuation of 60 dB, and values of α from 0 to 2 in steps of 0.5.

The window based on the IDFT methods will be used as a reference. The window recurrence approach and the series computation give similar results. For small N, (23,24) the maximum difference in the normalized window coefficients is of the order 10^{-15}, for (239,240) of the order 10^{-13}, and for (1023,1024) of the order 10^{-12}.

As to the spectral match at N equally spaced frequency values (normalized to unity at $\omega = 0$) for $\alpha = 0$ and $\alpha = 1$, the differences are of the same magnitude as for the window samples for all

[11] The `gammaln` function can be used in MATLAB.

[12] Windows with such lengths are routinely used in audio processing – at a sampling rate of 48 kHz, a window length of 1024 corresponds to a duration of about 21 ms.

three approaches.

Table 2 shows the relative times for calculating windows.

Table 2 Relative Window Calculation Times

Window Calculation	$N = 240$ Time	$N = 1024$ Time
IDFT	1.79	19.94
Modified Recurrence	1.03	4.95
Series	3.37	123.17

3.6 Parameters of the Ultraspherical Windows

The parameter α changes the type of window and within each type of window, the parameter x_0 trades off main lobe width against sidelobe attenuation. The parameter α can be used to choose the rate of decrease (or increase) in sidelobe attenuation from sidelobe to sidelobe. For $\alpha = 0$ (Dolph-Chebyshev window), all sidelobes have the same height. For $\alpha > 0$, the sidelobe heights decrease with frequency. For $\alpha < 0$, the sidelobe heights increase with frequency. Also for $\alpha < 0$, not all of the window coefficients are necessarily of the same sign.

3.6.1 Designs for a fixed main lobe width

A set of ultraspherical windows with $N = 240$ was generated for different values of α from 0 to 2 in steps of 0.5. All of the windows were designed with $\sigma = 2$, corresponding to a main lobe width of $4/N$ Hz ($8\pi/N$ on the ω scale) – the same as for a Hann window. Figure 4 shows the frequency response of the window on a dB scale. In the first sidelobe, the Dolph-Chebyshev ($\alpha = 0$) has the lowest response and all sidelobes have the same height at -46.6 dB. The window designed with $\alpha = 2$ has the highest first sidelobe level of -35.2 dB, but subsequent sidelobes diminish quickly in height.

The windows are plotted in Fig. 5. Two of the windows ($\alpha = 0$ and $\alpha = 0.5$) have spikes at each end – the end samples are marked with circles. The uppermost curve is for the Dolph-Chebyshev window ($\alpha = 0$). If the elevated end-points are ignored, the windows are seen to be sitting on pedestals, with the size of the pedestal decreasing as α increases. It is remarkable that rather small changes in the shapes of the windows result in large changes in the frequency response, at least when plotted with a log amplitude.

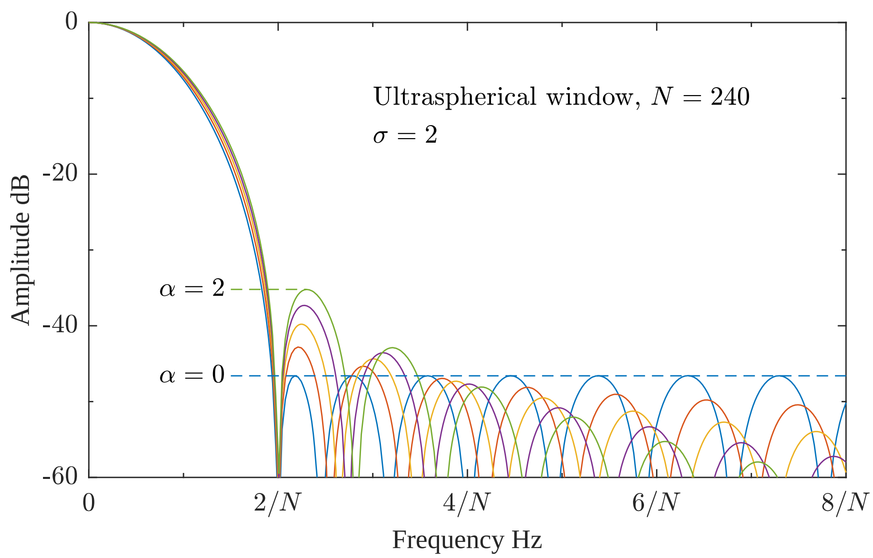

Fig. 4 Frequency responses for ultraspherical windows with $N = 240$ and a main lobe width of $4/N$ Hz ($\sigma = 2$). The values for α are [0, 0.5, 1, 1.5, 2]. The first sidelobe heights from bottom to top are in the same order as the α values.

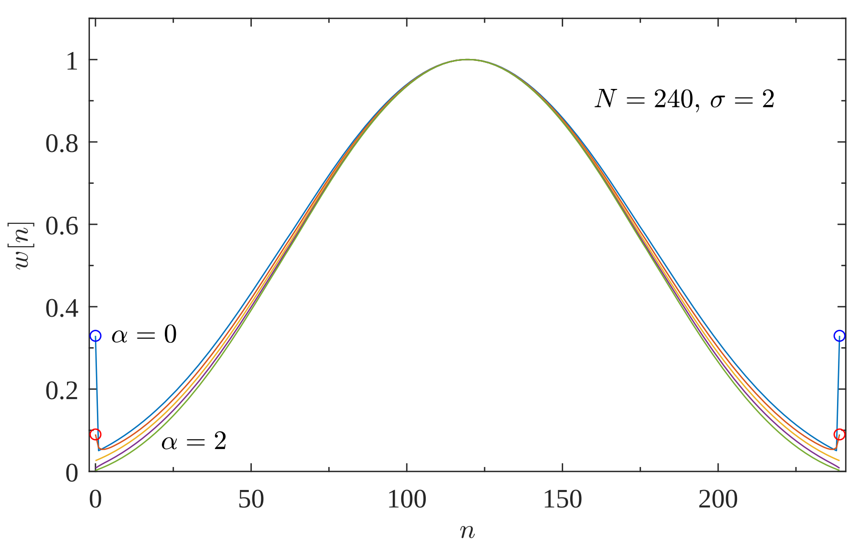

Fig. 5 A plot of the ultraspherical windows with $N = 240$ and a main lobe width of $4/N$ Hz ($\sigma = 2$). The values for α are [0, 0.5, 1, 1.5, 2]. The edges of the windows from top to bottom are in the same order as the α values. The upturned end points for $\alpha = 0$ and $\alpha = 0.5$ are marked with circles.

3.6.2 Design to minimize sidelobe energy

A design to control the *peak* value of the sidelobes was described earlier. A related approach controls the fraction of the energy in the sidelobes. A window based on a discrete prolate spheroidal sequence (DPSS) minimizes the fraction of the energy above a frequency W Hz. The determination of a DPSS window requires solving an eigenvalue problem.

Saramäki [9] shows that a window based on a Chebyshev polynomial of the second kind (an ultraspherical polynomial with $\alpha = 1$) is a good match to a DPSS window – slightly better than a Kaiser-Bessel window. A Kaiser-Bessel window is formed by sampling a continuous-time window which is a special case of the continuous-time ultraspherical windows discussed later. Rowińska-Schwarzweller and Wintermantel [15] show that for one of the examples used by Saramäki [9], an ultraspherical window with $\alpha = 0.8$ does an even better at matching a DPSS window. In this section, the extra flexibility of choosing the value of α to match DPSS windows is explored.

Fix the window length N. A set of values of main lobe widths was chosen – the values of σ run from 1 to 4. These will be the abscissa values for comparisons. DPSS windows are indexed by a time-bandwidth parameter NW. For each value of σ, a search procedure was used to find the value of NW which results in the main lobe width of the DPSS window being equal to σ. For each value of σ, an ultraspherical window was designed. The value of α for that window was optimized to minimize the mean squared error[13] between the ultraspherical window and the DPSS window with the same value of σ.

The results for $N = 240$ are shown in Fig. 6. The top plot shows the value of NW for the DPSS window. The middle plot shows the value of α for the ultraspherical window which gives the best match. The bottom plot shows the sidelobe attenuation factor R for the ultraspherical window with the optimized value of α.

Note that an ultraspherical window with $\alpha = 1$ and $\sigma = 1$ is a rectangular window. A DPSS window with $NW = 0$ is also a rectangular window. The root mean squared (RMS) error is zero for that case. The RMS error for the Saramäki window ($\alpha = 1$) is of the order 10^{-3} for $\sigma > 1$. The RMS error for the ultraspherical window with the optimized α is less than that for the Saramäki window by an increasing factor for increasing σ. For example for $\sigma = 2$, the RMS error for the Saramäki window is 1.511×10^{-3} and the RMS error for the optimized window is 0.411×10^{-3}.

Tests were also conducted with a short window with $N = 24$. The corresponding plots for NW and R are very similar. The optimal value of α is dependent on N. For the smaller N, α ranges from 1 to 0.7 instead of from 1 to 0.8. Tests with a larger $N = 480$ show that the graph of the optimal α tracks closely with that for $N = 240$.

[13] The error between a reference window $\mathbf{x}$ and a test window $\mathbf{y}$ is $\mathbf{e} = \mathbf{x} - a\mathbf{y}$, where the scaling factor $a = \mathbf{y}^T\mathbf{x}/(\mathbf{x}^T\mathbf{x})$ minimizes the average squared error $\mathbf{e}^T\mathbf{e}/N$. The root mean squared (RMS) error is $\sqrt{\mathbf{e}^T\mathbf{e}/N}$.

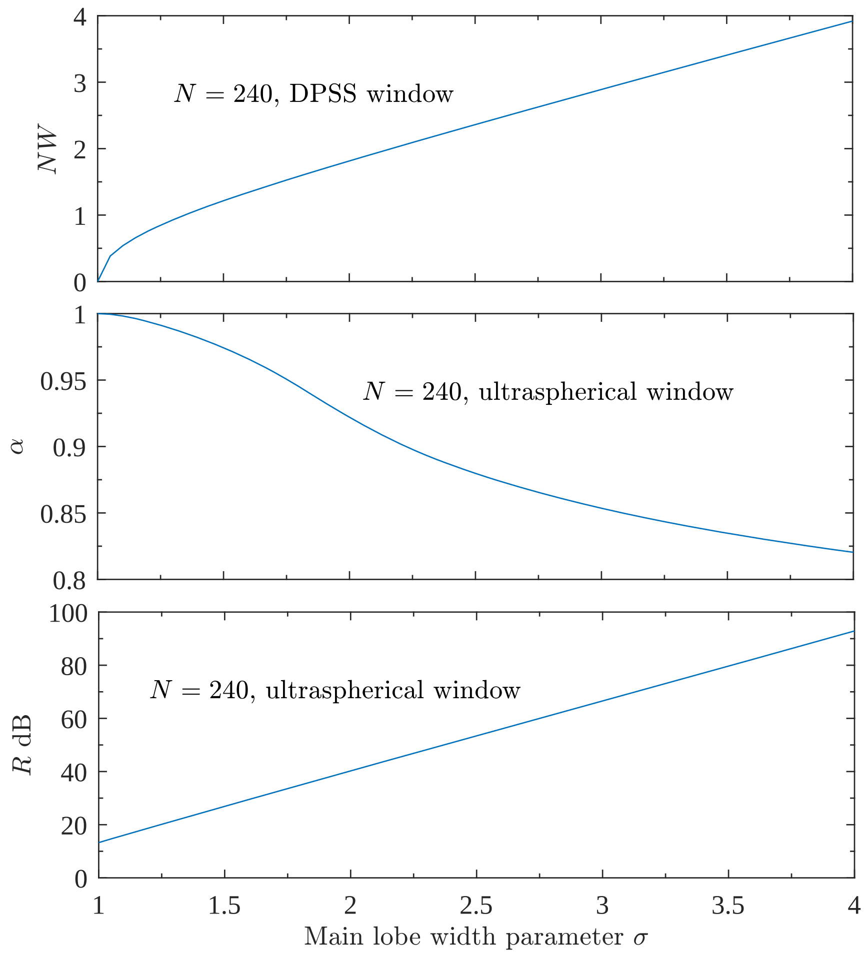

Fig. 6 Parameters of an ultraspherical window which is a best match to a DPSS window with $N = 240$. The abscissa for all plots is the main lobe width parameter σ, where $\sigma = 1$ is the main lobe width for a rectangular window. The top plot is the value of the time-bandwidth product NW for a DPSS window with the corresponding value of σ. The middle plot is the value of α which gives an ultraspherical window best matched to the DPSS window. The bottom plot is the sidelobe attenuation factor R for the ultraspherical window.

Figure 7 shows the frequency response of the DPSS window and the optimized ultraspherical window for $N = 240$ and $\sigma = 2$. The two curves are very close. If the Saramäki window ($\alpha = 1$) were to be added to the plot, it would be a good match to the DPSS window, but would not overlay the DPSS window as closely as the optimized window.

The DPSS window minimizes the energy for frequencies greater that W relative to the energy over all frequencies. The value of W is shown in Fig. 7 as a vertical line. Note that the frequencies lying above W include part of the main lobe as well as the sidelobes. As the DPSS parameter

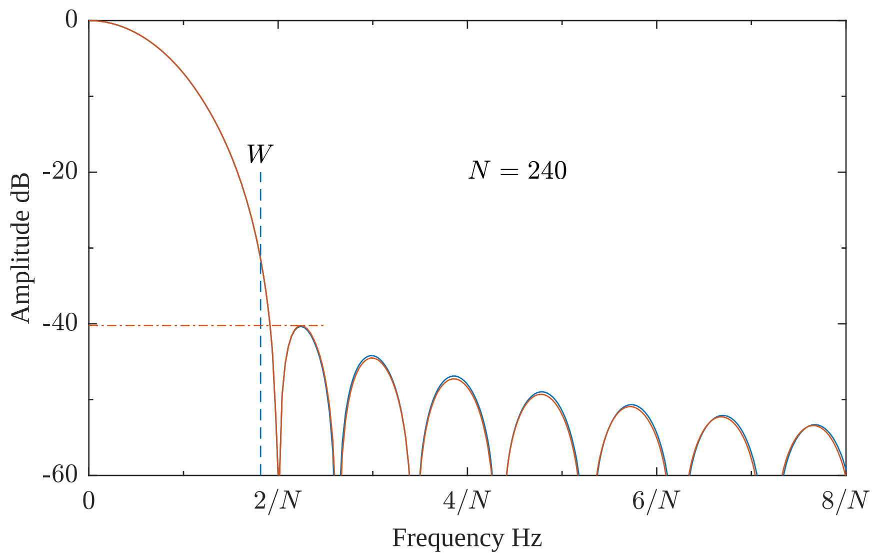

Fig. 7 Frequency responses of a DPSS window with $NW = 1.814$ and an ultraspherical window with $\alpha = 0.922$. Both windows have $N = 240$ and $\sigma = 2$ (corresponding to the null in the amplitude at $2/N$). The vertical line indicates the value of $W = 1.814/N$ for the DPSS window. The horizontal line marks the height of the first sidelobe of the ultraspherical window, which is $R = 40.2$ dB below the peak of the main lobe.

NW increases from 0, the fraction of the energy in frequencies below W increases from 0 to reach 99.98% when $\sigma = 2$. This large energy concentration factor may seem unlikely based on a plot of the spectrum win a logarithmic amplitude scale – a plot of the energy with a linear vertical scale shows otherwise.

A DPSS window treats all energy above W equally. But windows are often applied to signals for which the response drops off for higher frequencies. Then a window that better suppresses the first few sidelobes at the expense of less suppression for the other sidelobes may be preferred. The marginally better match to DPSS windows for windows with an optimized α may not have much practical utility relative to the Saramäki window. Further, the simplicity of dynamically implementing Kaiser-Bessel filters (see §5.3) which also approximate DPSS windows may win out over Saramäki windows.

4 Continuous-Time Ultraspherical Windows

The frequency response of a discrete-time ultraspherical window is found by evaluating an ultraspherical polynomial. In Streit [5], the order of the polynomial is allowed to grow without bound, to give the frequency response of continuous-time ultraspherical windows. For $\alpha > 1/2$,

$$W_c(\Omega) = \begin{cases} D(\beta,\alpha)\dfrac{I_{\alpha-1/2}\Bigl(\sqrt{\beta^2-\Omega_T^2}\Bigr)}{\Bigl(\sqrt{\beta^2-\Omega_T^2}\Bigr)^{\alpha-1/2}} & |\Omega_T| < \beta, \\ \dfrac{D(\beta,\alpha)}{D(0,\alpha)}, & |\Omega_T| = \beta, \\ D(\beta,\alpha)\dfrac{J_{\alpha-1/2}\Bigl(\sqrt{\Omega_T^2-\beta^2}\Bigr)}{\Bigl(\sqrt{\Omega_T^2-\beta^2}\Bigr)^{\alpha-1/2}} & |\Omega_T| > \beta, \end{cases} \tag{41}$$

where $\Omega_T = \Omega T/2$ and

$$D(\beta,\alpha) = \begin{cases} 2^{\alpha-1/2}\,\Gamma(\alpha+1/2), & \beta = 0, \\ \dfrac{\beta^{\alpha-1/2}}{I_{\alpha-1/2}(\beta)}, & \beta > 0. \end{cases} \tag{42}$$

This response has been normalized to give $W_c(0) = 1$. This expression avoids the use of complex arithmetic – the first part uses the modified Bessel function of the first kind (with the quantity inside the square root being positive), while the last part uses the ordinary Bessel function of the first kind (with the quantity inside the square root flipped so it is positive).[14] If $\alpha > 1/2$, the middle case ($|\Omega_T| = \beta$), results in an indeterminate $0/0$ form. The value for the middle case is given by the limit,

$$\lim_{\Omega_T \to \beta} W_c(\Omega) = \frac{D(\beta,\alpha)}{2^{\alpha-1/2}\,\Gamma(\alpha+1/2)}. \tag{43}$$

Separately, if $\alpha > 1/2$, the limit for $D(\beta,\alpha)$ as β goes to zero is

$$\lim_{\beta \to 0} D(\beta,\alpha) = 2^{\alpha-1/2}\,\Gamma(\alpha+1/2). \tag{44}$$

If $\alpha \leq 1/2$, the frequency response at $|\Omega_T| = \beta$ does not have to be drawn out as a separate case, see for example the case of $\alpha = 0$ shown below.

In [5], the frequency response of the CT (continuous-time) window is manipulated to express it as the Fourier transform of the window. The resulting CT windows (normalized to unit height

[14] The relationship between the modified and ordinary Bessel functions is $J_\alpha(jx) = j^\alpha I_\alpha(x)$ for real x [16, §9.6].

at $t = 0$ and length T) are [15]

$$\widetilde{w}(t) = \begin{cases} \left(\sqrt{1-(2t/T)^2}\right)^{\alpha-1} \dfrac{I_{\alpha-1}\left(\beta\sqrt{1-(2t/T)^2}\right)}{I_{\alpha-1}(\beta)}, & -T/2 \leq t \leq T/2, \\ 0, & \text{elsewhere.} \end{cases} \tag{45}$$

This formulation applies for $\alpha > 0$. As $\beta \to 0$, $\widetilde{w}(t) = \left(1-(2t/T)^2\right)^{\alpha-1}$. As $t \to \pm T/2$, the end points of the window take on the value $0^{\alpha-1}$, i.e., 0, 1, or ∞ depending on the value of α.[16]

$\alpha > 1$: the window is bell-shaped and the end points are zero.

$\alpha = 1$: the window is constant for $\beta = 0$ and becoming bell-shaped as β increases, but with the end points of the window being non-zero.

$0 < \alpha < 1$: the end points become infinite – the window is bell-shaped in the middle, but the ends of the window are upturned, shooting off to infinity at $t = \pm T/2$.

$\alpha = 0$: the window has a smooth part which for $\beta > 0$ is bell-shaped with non-zero end points, together with with Dirac delta functions at the end points. The expression for the window when $\alpha = 0$ is given below.

The CT ultraspherical windows have a frequency response *and* a time window given by closed-form expressions in terms of Bessel functions.

CT Dolph-Chebyshev window, $\alpha = 0$

The frequency response of the CT Dolph-Chebyshev window can be obtained by specializing Eq. (41) for $\alpha = 0$. With $\Omega_T = \Omega T/2$, the result is[17]

$$W_c(\Omega) = \begin{cases} \dfrac{\cosh\left(\sqrt{\beta^2 - \Omega_T^2}\right)}{\cosh(\beta)}, & |\Omega_T| \leq \beta, \\ \dfrac{\cos\left(\sqrt{\Omega_T^2 - \beta^2}\right)}{\cosh(\beta)}, & |\Omega_T| \geq \beta. \end{cases} \tag{46}$$

[15]Streit gives the Fourier transform of the CT ultraspherical window in Eq. (60). Changing notation, $\tau \to \beta$, $v \to \Omega$, $\mu \to \alpha$, $\xi \to t$, and $L \to 2$,

$$H(\Omega) = C(\alpha,\beta) \int_{-1}^{1} \left(\sqrt{1-t^2}\right)^{\alpha-1} I_{\alpha-1}\left(\beta\sqrt{1-t^2}\right) \cos(\Omega t)\, dt,$$

where $C(\alpha,\beta)$ gathers up terms that do not depend on t. Then $h(t)$ is the product of $C(\alpha,\beta)$ and the terms before the cosine inside the integral.

[16]The values for $\beta = 0$ and $t = \pm T/2$ are easily found using the series expansion in Appendix C.

[17]For $\alpha = 0$, the frequency dependent terms of Eq. (41) are of the form $\sqrt{z}\, I_{-1/2}(z)$. The Bessel function $I_{-1/2}(z)$ can be be expressed in terms of $\cosh(z)/\sqrt{z}$ [16, §10.2], resulting in the cancellation of the $\sqrt{z}$ terms.

This response has been normalized so that the response at $\Omega = 0$ (first part of the equation) is one. In the second part of the equation, the sidelobes have a constant peak magnitude of $1/\cosh(\beta)$. The ratio of the main lobe to the sidelobes is $R = \cosh(\beta)$. Inverting this equation, β can be determined from the sidelobe attenuation factor,

$$\beta = \cosh^{-1}(R). \tag{47}$$

The main lobe width can be determined from the second part of the equation. The first zero crossing occurs when $\sqrt{\Omega_T^2 - \beta^2} = \pi/2$. This zero occurs at[18]

$$\Omega_z = \frac{\pi}{T}\sqrt{1 + (2\beta/\pi)^2}. \tag{48}$$

Let σ be the ratio of the main lobe width to that of a rectangular window of length T,

$$\sigma = \frac{\Omega_z}{2\pi/T}. \tag{49}$$

Then σ and β are related as

$$\sigma = \frac{1}{2}\sqrt{1 + (2\beta/\pi)^2}; \qquad \beta = \frac{\pi}{2}\sqrt{4\sigma^2 - 1}. \tag{50}$$

The main lobe width is equal to that of a rectangular window ($\sigma = 1$) when $\beta = \pi\sqrt{3/4} \approx 2.72074$ and equal to that of a Hann window ($\sigma = 2$) when $\beta = \pi\sqrt{15/4} \approx 6.0837$.

The inverse Fourier transform of Eq. (46) is ill-defined. Following Taylor [17], the frequency response of a CT Dolph-Chebyshev window can be decomposed into a first part which corresponds to a smooth time function, and a second part which adds delta functions in the time domain,

$$W_c(\Omega) = W_{cs}(\Omega) + W_{cp}(\Omega), \tag{51}$$

where the frequency response of the smooth part is

$$W_{cs}(\Omega) = \begin{cases} \dfrac{\cosh\left(\sqrt{\beta^2 - \Omega_T^2}\right) - \cos(\Omega_T)}{\cosh(\beta)}, & |\Omega_T| \le \beta, \\[2ex] \dfrac{\cos\left(\sqrt{\Omega_T^2 - \beta^2}\right) - \cos(\Omega_T)}{\cosh(\beta)}, & |\Omega_T| \ge \beta, \end{cases} \tag{52}$$

[18] The full set of zeros of the frequency response are $\Omega = \pm(\pi/T)\sqrt{(2k-1)^2 + (2\beta/\pi)^2}$, for $k = 1, 2, \ldots$.

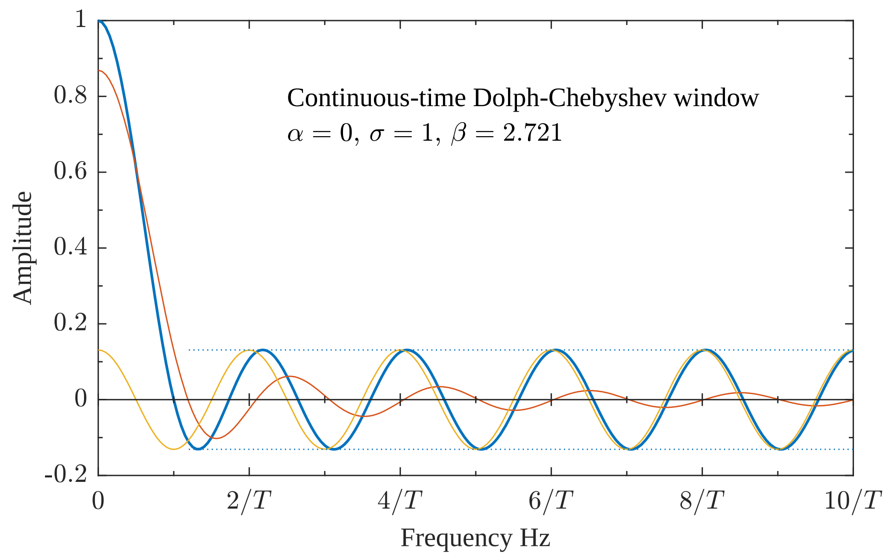

Fig. 8 Frequency response of a continuous-time Dolph-Chebyshev window with $\sigma = 1$ ($\beta = 2.721$). The thick line is the equiripple frequency response $W(\Omega)$ of the window. It is the sum of the response with decaying sidelobes $W_{cs}(\Omega)$ and the constant amplitude sinusoidal response $W_{cp}(\Omega)$.

and the frequency response due to the delta functions is

$$W_{cp}(\Omega) = \frac{\cos(\Omega_T)}{\cosh(\beta)}. \tag{53}$$

At $\Omega = 0$, the ratio of the $W_{cs}(0)$ to $W_{cp}(0)$ is $\cosh(\beta) - 1$, or equivalently $R - 1$.

Figure 8 shows the two components of the frequency response on a linear amplitude scale adding together. The window was designed with $\sigma = 1$, giving $\beta = 2.721$ and resulting in a sidelobe attenuation of $R = 7.628$ (17.65 dB).

Taylor invokes a Fourier transform relation [18, Pair 871.2] to compute the smooth part of the window. Adopting our notation, the smooth part of the unnormalized window is[19]

$$w_s(t) = \begin{cases} \dfrac{\beta}{T\cosh(\beta)} \dfrac{I_1\Big(\beta\sqrt{1-(2t/T)^2}\Big)}{\sqrt{1-(2t/T)^2}}, & -T/2 \le t \le T/2, \\ 0, & \text{elsewhere.} \end{cases} \tag{54}$$

Notice that the smooth part vanishes for $\beta = 0$. The delta functions at the ends of the unnormalized window are given by

$$w_d(t) = \frac{1}{2\cosh(\beta)} \delta(|t| - T/2). \tag{55}$$

For later convenience, the two terms forming the CT Dolph-Chebyshev window can be scaled to give,

$$w(t) = \begin{cases} \beta \dfrac{I_1\Big(\beta\sqrt{1-(2t/T)^2}\Big)}{\sqrt{1-(2t/T)^2}} + \dfrac{T}{2}\delta(|t| - T/2), & -T/2 \le t \le T/2, \\ 0, & \text{elsewhere.} \end{cases} \tag{56}$$

The ratio of the area of the smooth part of the window to the area of the delta function terms is equal to $R - 1$.

When $|t| = T/2$, the smooth part of the window takes on a value of $\beta/\big(2I_1(\beta)\big)$ times its value at $t = 0$. This ratio decreases monotonically from 1 as β increases from 0. When $\beta > 0$, the window can be normalized by the value $w(0)$.

---

[19]With $p = j2\pi f$, the Fourier transform pair 871.2 as given in [18] is

$$\cosh\big(a\sqrt{p^2 - \lambda^2}\big) - \cosh(ap) \Longleftrightarrow -\frac{a\lambda J_1(\lambda\sqrt{a^2 - g^2})}{2\sqrt{a^2 - g^2}}.$$

Let $a = T/2$, $a\lambda = j\beta$, $ap = j\Omega_T$,and $g = t$. Using $\cosh(j\Omega_T) = \cos(\Omega_T)$ and $J_1(jx) = jI_1(x)$,

$$\cosh\big(\sqrt{\beta^2 - \Omega_T^2}\big) - \cos(\Omega_T) \Longleftrightarrow \frac{\beta}{T} \frac{I_1(\beta\sqrt{1 - (2t/T)^2})}{\sqrt{1 - (2t/T)^2}}.$$

CT Kaiser-Bessel window, $\alpha = 1$

The frequency response of the Kaiser-Bessel window, with $\Omega_T = \Omega T/2$, is[20]

$$W_c(\Omega) = \begin{cases} D(\beta)\dfrac{\sinh\left(\sqrt{\beta^2 - \Omega_T^2}\right)}{\sqrt{\beta^2 - \Omega_T^2}}, & |\Omega_T| < \beta, \\ D(\beta), & |\Omega_T| = \beta, \\ D(\beta)\dfrac{\sin\left(\sqrt{\Omega_T^2 - \beta^2}\right)}{\sqrt{\Omega_T^2 - \beta^2}}, & |\Omega_T| > \beta, \end{cases} \tag{57}$$

where

$$D(\beta) = \begin{cases} 1, & \beta = 0, \\ \dfrac{\beta}{\sinh(\beta)}, & \beta > 0. \end{cases} \tag{58}$$

Using this form of the frequency response, the main lobe width and the relative level of the first sidelobe can be determined [19]. The frequency response of interest is the last case in Eq. (57) and is given in the form of a sinc function, $\operatorname{sinc}(\theta) = \sin(\theta)/\theta$. The first zero of the $\operatorname{sinc}(\theta)$ function occurs when $\theta = \pi$. Setting $\sqrt{\Omega_T^2 - \beta^2} = \pi$, gives the zero crossing as

$$\Omega_z = \frac{\pi}{T}\sqrt{1 + (\beta/\pi)^2}. \tag{59}$$

The main lobe width in radians is twice Ω_z. The term in the square root is the ratio of the main lobe width of the window to that of a rectangular window,

$$\sigma = \sqrt{1 + (\beta/\pi)^2}; \qquad \beta = \pi\sqrt{\sigma^2 - 1}. \tag{60}$$

Note that there is no real value of β which results in $\sigma < 1$.

The derivative of $\operatorname{sinc}(\theta)$ is $(\theta\cos(\theta) - \sin(\theta))/\theta^2$. The peaks of the sidelobes occur when the derivative is zero, i.e., when $\theta = \tan(\theta)$. The (negative-valued) peak of the first sidelobe occurs for θ above π but below $3\pi/2$. Solving the transcendental equation gives $\theta \approx 4.49341$ (1.4303π).[21]

---

[20] For $\alpha = 1$, the frequency dependent terms of Eq. (41), are of the form $I_{1/2}(z)/\sqrt{z}$. The Bessel function $I_{1/2}(z)$ can be be expressed in terms of $\sinh(z)/\sqrt{z}$ [16, §10.2], resulting in the final form $\sinh(z)/z$.

[21] Using MATLAB, a more accurate value can be obtained as

```
theta = fzero(@(theta)(tan(theta)-theta), [pi+eps,3*pi/2-eps]).
```

The resulting value is 4.493409457909062.

Then the main lobe (amplitude 1) to sidelobe amplitude ratio is

$$R = \frac{\sinh(\beta)}{\beta} \frac{1}{|\cos(\theta)|}, \tag{61}$$

where $1/|\cos(\theta)| \approx 4.60334$. This value corresponds to a sidelobe attenuation of 13.2615 dB, which is the sidelobe attenuation of a rectangular window ($\beta = 0$). Conversely, the value of β for a given R can be determined from the transcendental equation,[22]

$$\sinh(\beta) = \beta R |\cos(\theta)|. \tag{62}$$

For $\alpha = 1$, the window is the Kaiser-Bessel window. This window is the CT version of the discrete-time Saramäki window based on the Chebyshev polynomials of the second kind. The normalized window is

$$\tilde{w}(t) = \begin{cases} \dfrac{I_0\Big(\beta\sqrt{1-(2t/T)^2}\Big)}{I_0(\beta)}, & -T/2 \le t \le T/2, \\ 0, & \text{elsewhere.} \end{cases} \tag{63}$$

The Kaiser-Bessel window becomes rectangular for $\beta = 0$.

4.1 Series Expansion for CT Ultraspherical Windows

Appendix C expresses the values of a CT ultraspherical window in terms of a modified Bessel function $I_\nu(x)$. Incorporating the series expansion of the Bessel function gives a formula for a CT ultraspherical window. A normalized CT ultraspherical window is given by

$$\tilde{w}(t) = \big(1-(2t/T)^2\big)^{\alpha-1} \frac{S_{\alpha-1}\big(\beta^2(1-(2t/T)^2)\big)}{S_{\alpha-1}\big(\beta^2\big)}, \qquad -T/2 \le t \le T/2. \tag{64}$$

where the sum $S_\nu(z^2)$ is

$$S_\nu(z^2) = \sum_{k=0}^{\infty} s_k(z^2, \nu). \tag{65}$$

[22]For $R > 1/|\cos(\theta)|$, the value of β can be found using MATLAB as

```
beta = fzero(@(beta)(sinh(beta) - beta*R*abs(cos(theta))), [eps,50]).
```

The terms of the sum can be calculated recursively as

$$s_k(x,\nu) = \frac{x}{4k(\nu+k)} s_{k-1}(x,\nu), \qquad \text{for } k \geq 1 \text{ with } s_0(x,\nu) = 1. \tag{66}$$

The sum $S_\nu(z^2)$ can be calculated using only basic arithmetic operations. Note that the sum is equal to one when $z = 0$.

Dolph-Chebyshev window, $\alpha = 0$

Using the results of Appendix C, the series expansion for the CT Dolph-Chebyshev window is

$$w(t) = \frac{\beta^2}{2} S_1\big(\beta^2(1-(2t/T)^2)\big) + \frac{T}{2}\delta(|t| - T/2), \qquad -T/2 \leq t \leq T/2. \tag{67}$$

For $\beta = 0$, the window consists of only the delta functions. For $\beta > 0$, the window can be normalized by the value window at $t = 0$.

Saramäki window, $\alpha = 1$

The formulation in Eq. (118) is particularly efficient for $\alpha = 1$ ($\nu = 0$), since the term in front of the sum evaluates to unity.

$$w(t) = S_0\big(\beta^2(1-(2t/T)^2)\big), \qquad -T/2 \leq t \leq T/2. \tag{68}$$

5 Sampling Continuous-Time Ultraspherical Windows

Many standard windows are sampled versions of continuous-time windows. There is a question of where to place the samples of the continuous-time window. Consider a CT window $w(t)$ of length T where the non-zero values lie in the interval $[-T/2, T/2]$. A discrete-time window can be created by sampling this window at N uniformly spaced points from t_0 to t_{N-1}, where the end points of the sample times normally lie in the interval $[-T/2, T/2]$,

$$w[n] = w(t_0 + n\Delta t/2), \tag{69}$$

where the sampling interval is $\Delta t = (t_{N-1} - t_0)/(N-1)$. The sampled window is a one-sided window. It will be symmetric about its middle if the CT window is symmetric and $t_{N-1} = -t_0$.

Many textbooks on digital signal processing choose $t_{N-1} = -t_0 = T/2$. Then $\Delta t = T/(N-1)$. This choice will be designated as the *conventional sampling* pattern. For CT windows which are zero at the ends (for instance a CT ultraspherical window for $\alpha > 1$), the discrete-time window has $N-2$ non-zero samples.

Consider a *modified sampling* pattern, with $t_{N-1} = T/2 - \Delta t/2$ and $t_0 = -t_{N-1}$. Then $\Delta t = T/N$. Some continuous-time windows include sinusoidal terms which evolve through a multiple of a half period across the window. The Δt used in modified sampling ensures that the discrete-time window also has sinusoidal terms which evolve in step.

For symmetrical sampling, the sampling times are

$$t_n = \big(n - \frac{N-1}{2}\big)\Delta t. \tag{70}$$

This formulation subsumes both conventional and modified sampling patterns.[23]

5.1 Frequency Response of a Sampled Continuous-Time Window

The frequency response of the digital filter can be calculated directly from the window samples, but an analytic expression for the frequency response can give further insight. If a useful analytic expression is not available, one may be able to get insight from an analytic form of the frequency response of the continuous-time window.

Let the CT window be $w(t)$ with frequency response $W_c(\Omega)$ (where $\Omega = 2\pi F$). If this response

[23]The number of samples in the interval $[-T/2, T/2]$ is exactly N when

$$\frac{T}{N+1} < \Delta t \le \frac{T}{N-1}.$$

is sampled at $t_n = n\Delta t$, the frequency response of the discrete-time window is a frequency-aliased version of $W_c(\Omega)$ [20],

$$W(\omega) = \frac{1}{\Delta t} \sum_{m=-\infty}^{\infty} W_c\Big(\frac{\omega - 2\pi m}{\Delta t}\Big) \qquad -\pi \le \omega \le \pi. \tag{71}$$

Now shift $w(t)$ to become $w'(t) = w(t + t_0)$, so that the sample for $n = 0$ corresponds to $w(t_0)$. The shifted window $w'(t)$ has the frequency response $W'_c(\Omega) = \exp(j\Omega t_0) W_c(\Omega)$. Then sample $w'(t)$ at $t_n = n\Delta t$. If $t_0 = -\Delta t(N-1)/2$, the sampled window has the frequency response

$$W(\omega) = \frac{1}{\Delta t} e^{-j\omega \frac{N-1}{2}} \sum_{m=-\infty}^{\infty} (-1)^{m(N-1)} W_c\Big(\frac{\omega - 2\pi m}{\Delta t}\Big) \qquad -\pi \le \omega \le \pi. \tag{72}$$

If N is odd (there is a sample at $t = 0$), then $(-1)^{m(N-1)} = 1$. If N is even, then $(-1)^{m(N-1)} = (-1)^m$. This means that the aliasing terms add differently for N even and N odd. Note that $W(\omega)$ depends on Δt, accommodating conventional and modified sampling patterns. If $W_c(\Omega)$ falls off rapidly enough and the number of samples is large (N large gives Δt small), some or all of the aliasing terms ($m \neq 0$) can be ignored.

5.2 Sampled Continuous-Time Ultraspherical Windows

For the specific case of a continuous-time ultraspherical window, the end time samples taken at $|t| = T/2$ will be infinite for $0 < \alpha < 1$ and will be zero for $\alpha > 1$. Only for $\alpha = 1$ will the end samples be non-zero and finite. Modified sampling is called for. The case of $\alpha = 0$ is handled separately.

The samples of the CT ultraspherical window can be calculated using the series expansion derived in Appendix C. The computation time for the series calculation of the sampled CT ultraspherical window can be compared to that of the discrete-time ultraspherical window as shown in Table 3. The sampled CT window computation is much faster than the fastest discrete-time ultraspherical window.

Table 3 Relative Window Calculation Times

Window Calculation	$N = 240$ Time	$N = 1024$ Time
Sampled CT Window	0.02	0.06
IDFT	1.79	19.94
Modified Recurrence	1.03	4.95

Sampled CT Dolph-Chebyshev window, $\alpha = 0$

Following Taylor's analysis, a CT Dolph-Chebyshev window can be decomposed as the um of a smooth time function $w_s(t)$ and delta functions $w_d(t)$ at the ends of the window as given by Eq. (56). Sampling the smooth function is straightforward, but the delta functions require separate attention.

The delta functions in the CT window will be replaced by discrete-time pulses in the sampled window. The Fourier transform of the impulse functions in the CT window and the zero-phase frequency response of the discrete-time pulses used in the sampled window are compared below,

$$\begin{aligned} \frac{T}{2}\big[\delta(t-T/2)+\delta(t+T/2)\big] &\leftrightarrow T\cos(\Omega T/2), \\ c(\beta,T,N)\big[\delta[n]+\delta[n-(N-1)]\big] &\leftrightarrow 2c(\beta,T,N)\cos(\omega(N-1)/2). \end{aligned} \tag{73}$$

The cosine terms on the right sides of the equations are identical for all values of ω and Ω when $\Omega = \omega\Delta t$, where $\Delta t = T/(N-1)$. This value of Δt (corresponding to conventional sampling) will be the sampling interval for the smooth part of the CT window. The contribution of the discrete-time pulses in the second line above uses the scaling factor $c(\beta,T,N)$.

The goal is to set the correct ratio of the zero-phase frequency response of the sampled smooth part of the window $w_{sx}[n]$ and the response of the pulse contribution $w_{px}[n]$. These responses are $B_{sx}(\omega)$ and $B_{px}(\omega)$, respectively. At $\omega = 0$, this ratio is ideally the same as for the CT window, viz., $R-1$.

A first method for choosing $c(\beta,T,N)$ finds $B_{sx}(0)$ as the sum of the sampled smooth coefficients and $B_{px}(0)$ as the sum of the pulses. Equating the ratio $B_{sx}(0)/B_{px}(0)$ to $R-1$ and solving for $c(\beta,T,N)$ gives

$$c(\beta,T,N) = \frac{1}{2(R-1)}\sum_{n=0}^{N-1} w_{sx}[n]. \tag{74}$$

Note that the sum of the samples of the smooth window takes into account any aliasing that affects the value at $\omega = 0$.

A second approach ignores the aliasing at $\omega = 0$ and thus assumes that Eq. (71) applies with the aliasing terms ($m \neq 0$) absent. Note that in Eq. (71), the spectrum of a sampled window is given as the aliased spectrum of the CT window scaled by Δt. The pulse contribution should also be scaled by Δt. Neglecting the effect of aliasing at $\omega = 0$, the sampled window is

$$w[n] = \begin{cases} \beta\dfrac{I_1\Big(\beta\sqrt{1-\tau_n^2}\Big)}{\sqrt{1-\tau_n^2}} + \dfrac{N-1}{2}\big(\delta[n]+\delta[n-(N-1)]\big), & 0 \le n \le N-1, \\ 0, & \text{otherwise,} \end{cases} \tag{75}$$

where $\tau_n = 2t_n/T = -1 + 2n/(N-1)$. Using the series expansion from Appendix C for the first part of the window expression,

$$w[n] = \frac{\beta^2}{2} S_\nu\big(\beta^2(1-\tau_n^2)\big) + \frac{N-1}{2}\big(\delta[]n] + \delta]n - (N-1)]\big), \qquad 0 \le n \le N-1. \tag{76}$$

Above it is suggested that a conventional sampling pattern for the smooth part of the Dolph-Chebyshev window be used. It was verified that using a modified sampling pattern resulted in a poorer match to the reference discrete-time Dolph-Chebyshev window. It was also determined that using the second approach to setting the end elements of $w_{px}[n]$ to $(N-1)/2$ to control the spectrum at $\omega = 0$ is marginally better than setting them based on the sum of $w_{sx}[n]$. The formulation in Eq. (76) will be designated as the Match0 approach.

Appendix D outlines a scheme to give a sampled CT Dolph-Chebyshev window with a refined approximation to an equiripple response. This is achieved by using the end samples of the window to control the frequency response at both $\omega = 0$ and $\omega = \pi$. This strategy results in an almost equiripple behaviour in the sidelobes and will be designated as the Match0π approach.

The two different approaches were used for a sampled CT Dolph-Chebyshev window of length $N = 160$ with $\sigma = 2$. For the CT window, this corresponds to a sidelobe attenuation of 46.82 dB. Figure 9, shows the frequency response of the Match0π window as being almost equiripple with the sidelobe peaks very close to the dashed line at -46.82 dB. The difference between the largest and smallest sidelobe peaks is 0.03 dB. The second curve is the frequency response of the Match0 window and has a larger difference between the largest and smallest sidelobe peaks of 1.77 dB.

The example above was for N even. The Match0π approach uses an estimate of the value of x_0 in its calculations. For the example plotted in Fig. 9, setting x_0 to 1 gives substantially the same result. For an odd number of samples ($N = 161$), the peak-to-peak variations are essentially the same as for $N = 160$. .

Sampled CT Kaiser-Bessel window, $\alpha = 1$

Kaiser-Bessel windows are formed when the CT ultraspherical windows with $\alpha = 1$ are sampled. The Kaiser-Bessel window is normally created using the conventional sampling pattern. These windows are popular since the Bessel function $I_0(z)$ can be computed using a rapidly convergent series [19] [16, §9.6]. A more convenient form is the series expansion derived in Appendix C.

The report [2] shows that the modified sampling pattern gives a better match to the discrete-time Saramäki window (generated by the ultraspherical polynomial with $\alpha = 1$). For a given sidelobe attenuation, the modified Kaiser-Bessel window has a slightly smaller main lobe width than the conventional Kaiser-Bessel window.

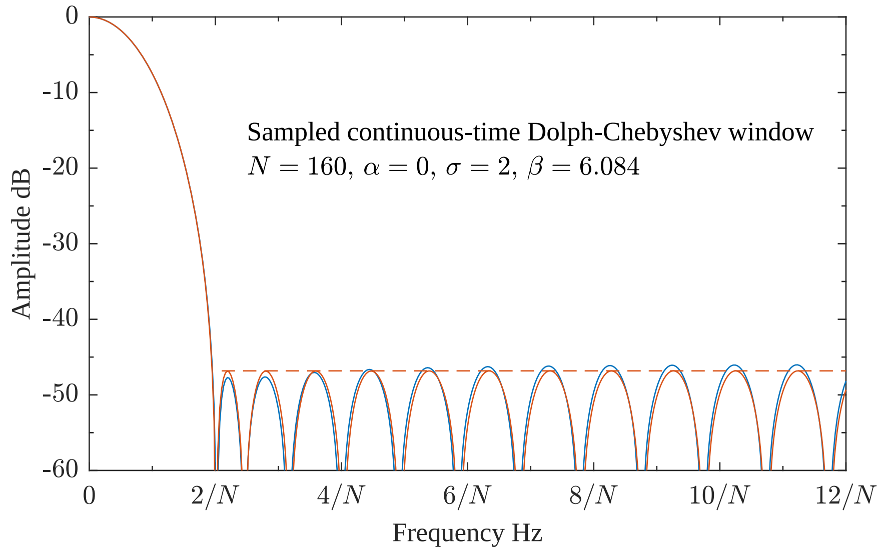

Fig. 9 Frequency response of a sampled continuous-time Dolph-Chebyshev windows with $N = 160$ and $\sigma = 2$ ($\beta = 6.084$). The nearly equiripple stopband response is for the window designed using the Match0π approach. The other curve is for a window designed using the Match0 approach.

5.3 Design to Minimize Sidelobe Energy

The Kaiser-Bessel windows were originally proposed as good approximations to DPSS windows. As in the case of the discrete-time windows described in §3.6.2 which approximate a DPSS windows, one can find the parameters of a CT ultraspherical window which best matches a given DPSS window. The optimal values of the α / β parameters for the CT window are plotted in Fig. 10. The optimal value of α for the CT window can be compared to that for the discrete-time ultraspherical window (Fig. 6). A plot of the corresponding value of R is indistinguishable from the value for discrete-time window and is not shown.

A plot of the spectral match for a CT ultraspherical window using an optimized value for α is shown in Fig. 11. This can be compared to Fig. 7 which shows the spectral match for a discrete-time ultraspherical window.

Table 4 shows the error between a DPSS window and different approximations. The values for window lengths $N = 240$ and $N = 24$ are shown. All windows are designed for a main lobe width given by $\sigma = 2$. For this value of σ, the time-bandwidth parameter of the DPSS window is about 1.81, The first line of results is for Kaiser-Bessel window (sampled CT window). The next line is for a Saramäki window. The third line is a sampled CT ultraspherical window with an optimized value for α. The bottom line is for a discrete-time ultraspherical window with an optimized value for α. The RMS error measures the error relative to the DPSS window. The sampled CT

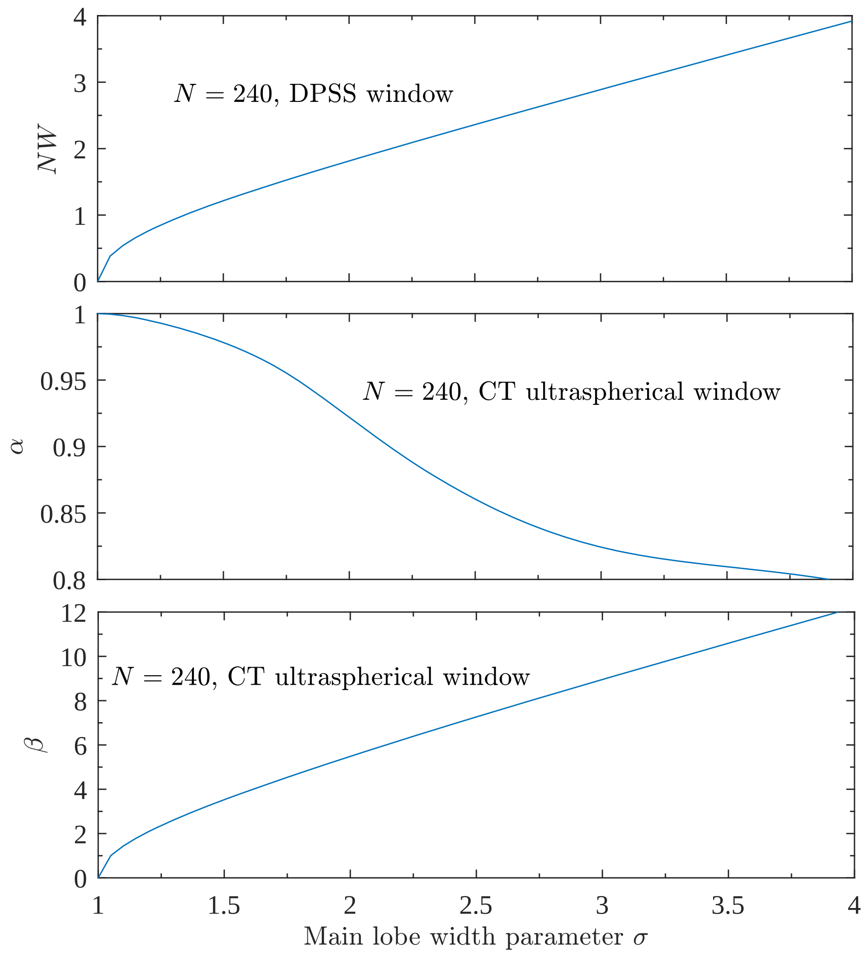

Fig. 10 Parameters of a CT ultraspherical window which is a best match to a DPSS window with $N = 240$. The abscissa for all plots is the main lobe width parameter σ, where $\sigma = 1$ is the main lobe width for a rectangular window. The top plot is the value of the time-bandwidth product NW for a DPSS window with the corresponding value of σ. The middle plot is the value of α which gives a CT ultraspherical window best matched to the DPSS window. The bottom plot is the value of β for the CT ultraspherical window with the main lobe width σ and the optimized value of α.

window with $\alpha = 1$ (Kaiser-Bessel window) and the sampled CT ultraspherical windows with an optimized value for α are shown in Table 4.

The windows with an optimized α have a significantly smaller RMS error than those with $\alpha = 1$. However any of the windows is a relatively good approximation to the DPSS window.

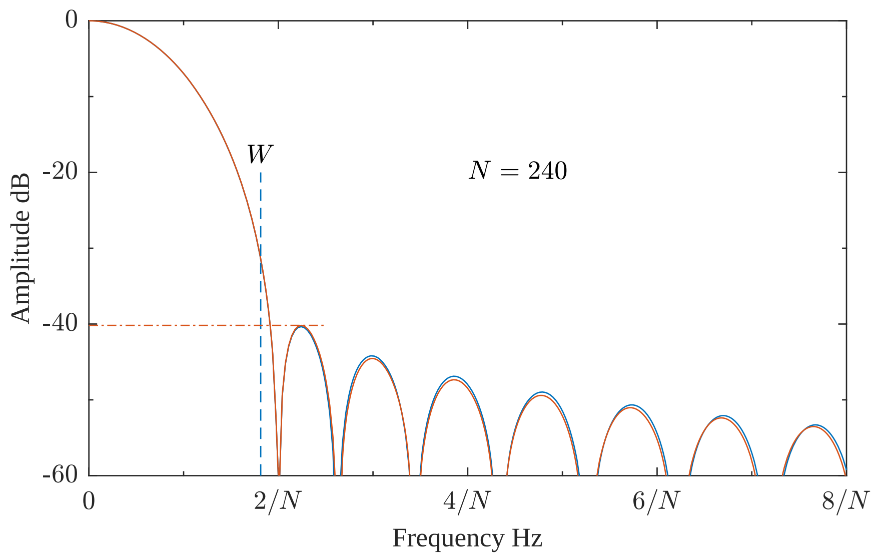

Fig. 11 Frequency responses of a DPSS window with $NW = 1.814$ and a sampled continuous-time ultraspherical window with $\beta = 5.48$ and $\alpha = 0.922$. Both windows have $N = 240$ and $\sigma = 2$ (corresponding to the null at frequency $2/N$). The vertical line indicates the value of $W = 1.814/N$ for the DPSS window. The horizontal line marks the height of the first sidelobe of the CT ultraspherical window, which is $R = 40.2$ dB below the peak of the main lobe.

Table 4 Match to a DPSS window with $\sigma = 2$

Window Type	$N = 24$		$N = 240$	
	α	RMS error	α	RMS error
Sampled CT window	1	4.225×10^{-3}	1	1.728×10^{-3}
Discrete-Time window	1	1.424×10^{-3}	1	1.509×10^{-3}
Sampled CT window	0.825	0.838×10^{-3}	0.922	0.570×10^{-3}
Discrete-Time window	0.878	0.183×10^{-3}	0.922	0.411×10^{-3}

6 Summary

This report has explored the calculation and design of discrete-time windows based on ultraspherical polynomials. The resulting windows are parameterized by the window length N and two other parameters. The first parameter α sets the window type which controls the rate at which the peaks of the sidelobes in the spectrum decrease (or increase). The window types include the Dolph-Chebyshev window ($\alpha = 0$) and the Saramäki window ($\alpha = 1$), but also a continuum between these two types and beyond ($\alpha > 1$).

The basic formulation involves first mapping the ultraspherical polynomial to a real (zero-phase) spectrum. Since the spectrum is that of a polynomial with N terms, the window coefficients are conveniently calculated using an inverse Discrete Fourier Transform of N samples of the spectrum. The computation of the IDFT is simplified by leveraging the symmetry and the realness of both the zero-phase spectrum and the resulting window.

New methods to calculate ultraspherical windows using a recurrence relationship are introduced. These use only basic arithmetic operation and avoid the need to use trigonometric functions. These are both precise and computationally efficient.

An alternate direct calculation of the window using a power series formulation advocated in the prior literature is shown to be problematic for large N unless modified to take into account the wide dynamic range of the combinatorial quantities involved.

The design of ultraspherical windows based on choosing the ratio of the main lobe peak to the first sidelobe peak, or based on the width of the main side lobe is described. The behaviour of the window and its spectrum for a fixed N and fixed main lobe width was presented, revealing the effect of changes in the window type.

This report has also included the formulation of continuous-time windows based on letting the order of the ultraspherical polynomial grow without bound. These continuous-time windows are a function of only two parameters, the window type α, and β which affects the trade-off between the main lobe width and the sidelobe attenuation. The formulas for the window and its spectrum are provided.

The formula for the continuous-time ultraspherical window is shown to be expressible as the sum of a rapidly converging series. Discrete-time windows can be formed by sampling the CT window. The use of the series expansion for samples of the CT window is appropriate for on-line computations, being more than an order of magnitude faster than the fastest algorithms for computing discrete-time ultraspherical windows.

For sampled continuous-time Dolph-Chebyshev windows, a novel procedure which sets the end points of the window provides a very good approximation to the equiripple behaviour of a discrete-time Dolph-Chebyshev window. This approach avoids the more onerous computation of the discrete-time Dolph-Chebyshev window.

Appendix A Ultraspherical Polynomial Recurrence

A.1 Basic Polynomial Recurrence

The ultraspherical recurrence relation in Eq. (1) can be written compactly as

$$C_m(x) = a_m x C_{m-1}(x) - b_m C_{m-2}(x), \qquad m \geq 2;\ C_0(x) = 1, C_1(x) = a_1 x, \tag{77}$$

where

$$a_m = 2 + 2\frac{\alpha - 1}{m};, \qquad b_m = 1 + 2\frac{\alpha - 1}{m}. \tag{78}$$

The polynomial $C_m(x)$ will have only even powers of x when m is even and only odd powers of x when m is odd.

Consider the recurrence for $m = 1$ and solve for $C_{-1}(x)$,

$$C_{-1}(x) = \frac{a_1}{b_1} x C_0(x) - \frac{1}{b_1} C_1(x) = 0. \tag{79}$$

Using this value allows for computation of the ultraspherical polynomial for $m \geq 1$, with the initial conditions $C_{-1}(x) = 0$ and $C_0(x) = 1$.

A.2 A Modified Recurrence

The ultraspherical polynomials of odd order have a zero for $x = 0$. Once the corresponding root factor is removed, the polynomial is of even order. Dividing by x renders the value of the lower order polynomial indeterminate at $x = 0$. An alternating recurrence relation can be formulated.

For m odd, define a lower order polynomial $C_m^\dagger(x)$ satisfying,

$$C_m(x) = x C_m^\dagger(x). \tag{80}$$

The initialization for the first odd order term is $C_1^\dagger(x) = a_1$. The subsequent alternating recurrences are

$$\begin{aligned} C_m(x) &= a_m x^2 C_{m-1}^\dagger(x) - b_m C_{m-2}(x), && m \text{ even}, \\ C_m^\dagger(x) &= a_m C_{m-1}(x) - b_m C_{m-2}^\dagger(x), && m \text{ odd}. \end{aligned} \tag{81}$$

There is no multiplication by x in the odd order recurrence and the multiplication by x^2 appears only in the even order recurrence. The even and odd recurrence relations alternate until $m = M$ is reached.

M even

If M is even, the result has used only even powers of x.

M odd

If M is odd, $C^{\dagger}_{M}(x)$ evaluates a $M-1$ order polynomial without the factor x. If the result of the Mth order (M odd) polynomial is needed, multiply by x as in Eq. (80). That result is a function of odd powers of x.

Dolph-Chebyshev / Saramäki windows, $\alpha = 0$ / $\alpha = 1$

The Dolph-Chebyshev and the Saramäki windows have the same recurrence relations, but differ in the initial values. For these windows, $a_m = 2$ and $b_m = 1$ for $m \geq 2$.

For the modified recurrence formulation, these fixed recurrence coefficients simplify the computations. An additional simplification occurs if $C^{\dagger}_{m}(x)$ satisfies

$$C_m(x) = 2xC^{\dagger}_{m}(x). \tag{82}$$

Then the modified recurrence relations become

$$\begin{aligned} C_m(x) &= 4x^2 C^{\dagger}_{m-1}(x) - C_{m-2}(x), \quad && m \text{ even}, \\ C^{\dagger}_{m}(x) &= C_{m-1}(x) - C^{\dagger}_{m-2}(x), && m \text{ odd}. \end{aligned} \tag{83}$$

If the final value of m is odd, apply Eq. (82) to get $C_m(x)$.

A.2.1 Polynomial coefficients

The modified recurrence can be used to calculate the coefficients corresponding to a direct form polynomial. When m is even, $\mathbf{p}_m$ is the vector of coefficients with elements $p_m[k]$ corresponding to the even powers x^{2k}. When m is odd, $\mathbf{q}_m$ is the vector of coefficients with elements $q_m[k]$ corresponding to the odd powers x^{2k+1}. In vector notation,

$$\mathbf{p}_m = \begin{bmatrix} p_m[0] \\ \vdots \\ p_m[m/2] \end{bmatrix}, \; m \text{ even}; \quad \mathbf{q}_m = \begin{bmatrix} q_m[0] \\ \vdots \\ q_m[(m-1)/2] \end{bmatrix}, \; m \text{ odd}. \tag{84}$$

The initial conditions are:

$$\mathbf{p}_0 = \begin{bmatrix} 1 \end{bmatrix}, \; \mathbf{q}_1 = a_1 \begin{bmatrix} 1 \end{bmatrix}. \tag{85}$$

The following recurrences alternate for $m = 2, \ldots, M$,

$$\begin{aligned}
\begin{bmatrix} \mathbf{p}_m \end{bmatrix} &= a_m \begin{bmatrix} 0 \\ \mathbf{q}_{m-1} \end{bmatrix} - b_m \begin{bmatrix} \mathbf{p}_{m-2} \\ 0 \end{bmatrix}, \quad m \text{ even, } m/2 \text{ values,} \\
\begin{bmatrix} \mathbf{q}_m \end{bmatrix} &= a_m \begin{bmatrix} \mathbf{p}_{m-1} \end{bmatrix} - b_m \begin{bmatrix} \mathbf{q}_{m-2} \\ 0 \end{bmatrix}, \quad m \text{ odd, } (m-1)/2 \text{ values.}
\end{aligned} \tag{86}$$

When $m = M$,

$$C_M(x) = \begin{cases} \displaystyle\sum_{k=0}^{M/2} p_M[k]\, x^{2k}, & M \text{ even,} \\ \displaystyle\sum_{k=0}^{(M-1)/2} q_M[k]\, x^{2k+1}, & M \text{ odd.} \end{cases} \tag{87}$$

A.3 Double-Step Recurrence

A double-step recurrence gives $C_m(x)$ in terms of $C_{m-2}(x)$ and $C_{m-4}(x)$. First use the basic ultraspherical recurrence twice to get

$$C_m(x) = a_m x\big(a_{m-1} x C_{m-2}(x) - b_{m-1} C_{m-3}(x)\big) - b_m C_{m-2}(x). \tag{88}$$

Express $C_{m-3}(x)$ as

$$C_{m-3}(x) = \frac{1}{a_{m-2} x}\big(C_{m-2}(x) + b_{m-2} C_{m-4}(x)\big). \tag{89}$$

Replacing $C_{m-3}^{(\alpha)}(x)$ with this expression and gathering terms gives a three term recurrence for $m \geq 4$,

$$C_m(x) = (f_m x^2 - g_m) C_{m-2}(x) - h_m C_{m-4}(x), \tag{90}$$

where

$$f_m = a_m a_{m-1}, \quad g_m = b_m + \frac{a_m b_{m-1}}{a_{m-2}}, \quad h_m = \frac{a_m b_{m-1}}{a_{m-2}} b_{m-2}. \tag{91}$$

The double-step recurrence for m even uses the initial values $C_0(x)$ and $C_2(x)$. For m odd, the initial values are $C_1(x)$ and $C_3(x)$, but as noted in §A.1, $C_{-1}(x)$ and $C_1(x)$ can be used instead.

Dolph-Chebyshev / Saramäki windows, $\alpha = 0$ / $\alpha = 1$

Using $a_m = 2$ and $b_m = 1$, the double-step recurrence for the Dolph-Chebyshev and the Saramäki windows is

$$C_m(x) = (4x^2 - 2) C_{m-2}(x) - C_{m-4}(x). \tag{92}$$

Appendix B Recurrence Formulation for Ultraspherical Window Coefficients

In this appendix recurrence relationships on the coefficient values are developed. For this, the ultraspherical polynomial is expressed as

$$C_m(z) = z^{m/2} \sum_{n=0}^{m} c_m[n] z^{-n}, \tag{93}$$

where $z = e^{j\omega}$. This expression is the zero-phase frequency response of an $m+1$ coefficient window.

The mapping from ω to x is $x(\omega) = x_0 \cos(\omega/2)$. In z-transform notation this is

$$x(z) = \frac{x_0}{2}\bigl(z^{1/2} + z^{-1/2}\bigr). \tag{94}$$

The following will also be useful,

$$x^2(\omega) = \frac{x_0^2}{2}\bigl(\cos(\omega) - 1\bigr), \tag{95}$$

giving

$$x^2(z) = \frac{x_0^2}{4}\bigl(z + 2 + z^{-1}\bigr). \tag{96}$$

B.1 Basic Ultraspherical Window Recurrence

The basic recurrence formula Eq. (77) is

$$C_m(x) = a_m x C_{m-1}(x) - b_m C_{m-2}(x). \tag{97}$$

Using the z-domain representation for $C_m(z)$, the recurrence is

$$z^{m/2} \sum_{n=0}^{m} c_m[n] z^{-n} = a_m x(z) z^{(m-1)/2} \sum_{n=0}^{m-1} c_{m-1}[n] z^{-n} - b_m z^{(m-2)/2} \sum_{n=0}^{m-2} c_{m-2}[n] z^{-n}. \tag{98}$$

After cancelling out the factor $z^{m/2}$,

$$\sum_{n=0}^{m} c_m[n] z^{-n} = a_m \frac{x_0}{2}(1 + z^{-1}) \sum_{n=0}^{m-1} c_{m-1}[n] z^{-n} - b_m z^{-1} \sum_{n=0}^{m-2} c_{m-2}[n] z^{-n}. \tag{99}$$

Equating terms in z^{-n}, the window coefficient vectors of length $m+1$ can be written as

$$\begin{bmatrix} \mathbf{c}_m \end{bmatrix} = a_m \frac{x_0}{2} \left\{ \begin{bmatrix} \mathbf{c}_{m-1} \\ 0 \end{bmatrix} + \begin{bmatrix} 0 \\ \mathbf{c}_{m-1} \end{bmatrix} \right\} - b_m \begin{bmatrix} 0 \\ \mathbf{c}_{m-2} \\ 0 \end{bmatrix}. \tag{100}$$

The initial conditions for the recurrence are

$$\mathbf{c}_0 = \begin{bmatrix} 1 \end{bmatrix}; \quad \mathbf{c}_1 = a_1 \frac{x_0}{2} \begin{bmatrix} 1 \\ 1 \end{bmatrix}. \tag{101}$$

B.2 Modified Window Recurrence

The modified recurrence relationships from §A.2 using $C_m(x) = xC_m^\dagger(x)$ are

$$\begin{aligned} C_m(x) &= a_m x^2 C_{m-1}^\dagger(x) - b_m C_{m-2}(x), \quad && m \text{ even}, \\ C_m^\dagger(x) &= a_m C_{m-1}(x) - b_m C_{m-2}^\dagger(x), && m \text{ odd}. \end{aligned} \tag{102}$$

***m* even**

Using the z-domain representation $C_m(z)$, the recurrence for m even is

$$z^{m/2} \sum_{n=0}^{m} c_m[n] z^{-n} = a_m x^2(z) z^{(m-2)/2} \sum_{n=0}^{m-2} \mathbf{c}_{m-1}^\dagger[n] z^{-n} - b_m z^{(m-2)/2} \sum_{n=0}^{m-2} c_{m-2}[n] z^{-n}. \tag{103}$$

After cancelling out the factor $z^{m/2}$,

$$\sum_{n=0}^{m} c_m[n] z^{-n} = a_m \frac{x_0^2}{4} (1 + 2z^{-1} + z^{-2}) \sum_{n=0}^{m-2} \mathbf{c}_{m-1}^\dagger[n] z^{-n} - b_m z^{-1} \sum_{n=0}^{m-2} c_{m-2}[n] z^{-n}. \tag{104}$$

In terms of the window coefficient vectors of length $m+1$,

$$\begin{bmatrix} \mathbf{c}_m \end{bmatrix} = a_m \frac{x_0^2}{4} \left\{ \begin{bmatrix} \mathbf{c}_{m-1}^\dagger \\ 0 \\ 0 \end{bmatrix} + 2 \begin{bmatrix} 0 \\ \mathbf{c}_{m-1}^\dagger \\ 0 \end{bmatrix} + \begin{bmatrix} 0 \\ 0 \\ \mathbf{c}_{m-1}^\dagger \end{bmatrix} \right\} - b_m \begin{bmatrix} 0 \\ \mathbf{c}_{m-2} \\ 0 \end{bmatrix}, \qquad m \text{ even}. \tag{105}$$

***m* odd**

For m odd, $C_m^\dagger(x)$ corresponds to a sequence $c_m^\dagger[n]$ of length $m-1$. The recurrence on the window coefficient vectors for m odd is

$$\sum_{n=0}^{m-1} c_m^\dagger[n] z^{-n} = a_m \sum_{n=0}^{m-1} c_{m-1}[n] z^{-n} - b_m z^{-1} \sum_{n=0}^{m-3} c_{m-2}^\dagger[n] z^{-n}. \tag{106}$$

The recurrence on the coefficient vectors of length $m-1$ is

$$\begin{bmatrix} \mathbf{c}_m^\dagger \end{bmatrix} = a_m \begin{bmatrix} \mathbf{c}_{m-1} \end{bmatrix} - b_m \begin{bmatrix} 0 \\ \mathbf{c}_{m-2}^\dagger \\ 0 \end{bmatrix}, \qquad m \text{ odd}. \tag{107}$$

If the final value for m is M and M is odd, the window coefficients are given by

$$\sum_{n=0}^{M} c_M[n] z^{-n} = \frac{x_0}{2}(1+z^{-1}) \sum_{n=0}^{M-1} c_M^\dagger[n] z^{-n} \tag{108}$$

In terms of window coefficients,

$$\begin{bmatrix} \mathbf{c}_M \end{bmatrix} = \frac{x_0}{2} \left\{ \begin{bmatrix} \mathbf{c}_M^\dagger \\ 0 \end{bmatrix} + \begin{bmatrix} 0 \\ \mathbf{c}_M^\dagger \end{bmatrix} \right\}, \qquad M \text{ odd}. \tag{109}$$

B.3 Double-Step Window Recurrence

Using the double-step recurrence of §A.3, the window recurrence can be written as

$$z^{m/2} \sum_{n=0}^{m} c_m[n] z^{-n} = \big(f_m x^2(z) - g_m\big) z^{(m-2)/2} \sum_{n=0}^{m-2} c_{m-2}[n] z^{-n} - h_m z^{(m-4)/2} \sum_{n=0}^{m-4} c_{m-4}[n] z^{-n} \tag{110}$$

Removing the factor $z^{m/2}$ in all terms gives

$$\sum_{n=0}^{m} c_m[n] z^{-n} = \big(f_m \frac{x_0^2}{4}(1+2z^{-1}+z^{-2}) - g_m z^{-1}\big) \sum_{n=0}^{m-2} c_{m-2}[n] z^{-n} - h_m z^{-2} \sum_{n=0}^{m-4} c_{m-4}[n] z^{-n}. \tag{111}$$

In terms of window coefficient vectors of length $m+1$,

$$\begin{bmatrix} \mathbf{c}_m \end{bmatrix} = f_m \frac{x_0^2}{4} \left\{ \begin{bmatrix} \mathbf{c}_{m-2} \\ 0 \\ 0 \end{bmatrix} + 2 \begin{bmatrix} 0 \\ \mathbf{c}_{m-2} \\ 0 \end{bmatrix} + \begin{bmatrix} 0 \\ 0 \\ \mathbf{c}_{m-2} \end{bmatrix} \right\} - g_m \begin{bmatrix} 0 \\ \mathbf{c}_{m-2} \\ 0 \end{bmatrix} - h_m \begin{bmatrix} 0 \\ 0 \\ \mathbf{c}_{m-4} \\ 0 \\ 0 \end{bmatrix}. \tag{112}$$

This procedure expresses an even/odd order window in terms of lower order even/odd order windows. The double-step window calculation was first described by Rowińska-Schwarzweller and Wintermantel in [15].

For m even, the recurrence starts with $\mathbf{c}_0$ and $\mathbf{c}_2$. For m odd, the recurrence starts with the initial conditions $\mathbf{c}_1$ and $\mathbf{c}_3$. Based on the discussion in §A.1, for $\alpha \neq 0$ the recurrence can be started at

$m = 1$ using the initial conditions for $m = -1$ and $m = 0$. Then the double-step recurrence can use an empty window vector for $m = -1$ and a two element window vector for $m = 1$. With a minor modification, these initial vectors can also be used for $\alpha = 0$.

Dolph-Chebyshev / Saramäki windows, $\alpha = 0$ / $\alpha = 1$

Using the double-step recurrence when $a_m = 2$ and $b_m = 1$, the double-step window recurrence becomes

$$\begin{bmatrix} \mathbf{c}_m \end{bmatrix} = x_0^2 \left\{ \begin{bmatrix} \mathbf{c}_{m-2} \\ 0 \\ 0 \end{bmatrix} + \begin{bmatrix} 0 \\ 0 \\ \mathbf{c}_{m-2} \end{bmatrix} \right\} + 2(x_0^2 - 1) \begin{bmatrix} 0 \\ \mathbf{c}_{m-2} \\ 0 \end{bmatrix} - \begin{bmatrix} 0 \\ 0 \\ \mathbf{c}_{m-4} \\ 0 \\ 0 \end{bmatrix}. \tag{113}$$

This formulation is the same as used by Saramäki in [9].[24]

[24]In [9], Eq.(20c) gives the double-step recurrence for an odd number of window coefficients with γ corresponding to x_0^2.

Appendix C Continuous-Time Ultraspherical Windows – Series Expansion

This appendix describes the calculation of continuous-time ultraspherical windows using a series expansion of the modified Bessel function.

C.1 Modified Bessel Function of the First Kind

First consider a series formula for calculating the modified Bessel function [16, §9.6]. For $\nu > -1$,

$$\begin{aligned} I_\nu(z) &= (z/2)^\nu \sum_{k=0}^{\infty} \frac{(z/2)^{2k}}{k!\,\Gamma(\nu+k+1)} \\ &= \frac{z^\nu}{2^\nu \Gamma(\nu+1)} \Big[1 + \sum_{k=1}^{\infty} \frac{z^{2k}}{4^k k!\,\Gamma(\nu+k+1)/\Gamma(\nu+1)} \Big]. \end{aligned} \tag{114}$$

Let the kth term in the sum be denoted by $s_k(x,\nu)$, where $x = z^2$. Then using the gamma function recursion $\Gamma(a+1) = a\Gamma(a)$ [16, §6.1] and the factorial recursion $k! = k(k-1)!$,

$$s_k(x,\nu) = \frac{x}{4k(\nu+k)} s_{k-1}(x,\nu), \qquad \text{for } k \geq 1 \text{ with } s_0(x,\nu) = 1. \tag{115}$$

The modified Bessel function becomes

$$I_\nu(z) = \frac{z^\nu}{2^\nu \Gamma(\nu+1)} S_\nu(z^2), \tag{116}$$

where

$$S_\nu(z^2) = \sum_{k=0}^{\infty} s_k(z^2,\nu). \tag{117}$$

The sum takes on the value 1 for $z = 0$, and each term in the sum is non-negative for $\nu > -1$. The first term in Eq. (116) determines the value at $z = 0$. The gamma function $\Gamma(\nu+1)$ is equal to the factorial $\nu!$ when ν is integer.

A practical procedure to calculate the value of the modified Bessel function entails recursively updating the partial sum and stopping when $s_k(z^2,\nu)$ falls below a threshold value. For instance, stop when $s_k(z^2,\nu)$ is less than ϵ times the partial sum. The value $\epsilon = 1 \times 10^{-8}$ was used in [21, §5.2] to calculate $I_0(z)$. For $\nu > -1$, each term $s_k(z^2,\nu)$ is non-negative and so the sum of the truncated series approaches the actual value from below.

C.2 Continuous-Time Ultraspherical Window

The continuous-time ultraspherical window is expressed in in terms of the modified Bessel function Eq. (45). Let $\nu = \alpha - 1$. Then for $-T/2 \leq t \leq T/2$,

$$\begin{aligned} w(t) &= \left(\sqrt{1-(2t/T)^2}\right)^{\nu} I_{\nu}\left(\beta\sqrt{1-(2t/T)^2}\right) \\ &= \frac{1}{2^{\nu}\Gamma(\nu+1)}\left(\sqrt{1-(2t/T)^2}\right)^{\nu}\left(\beta\sqrt{1-(2t/T)^2}\right)^{\nu} S_{\nu}\big(\beta^2(1-(2t/T)^2)\big) \\ &= \frac{\beta^{\nu}}{2^{\nu}\Gamma(\nu+1)}\big(1-(2t/T)^2\big)^{\nu} S_{\nu}\big(\beta^2(1-(2t/T)^2)\big). \end{aligned} \tag{118}$$

Note that the final form avoids the use of square roots.

The window can be normalized to give $\widetilde{w}(t) = w(t)/w(0)$, where

$$w(0) = \frac{\beta^{\nu}}{2^{\nu}\Gamma(\nu+1)} S_{\nu}(\beta^2). \tag{119}$$

The common leading terms in $w(t)$ and $w(0)$ cancel, even for $\beta = 0$. For $\beta = 0$ the sum term evaluates to one. The normalized form of the window is

$$\widetilde{w}(t) = \big(1-(2t/T)^2\big)^{\nu} \frac{S_{\nu}\big(\beta^2(1-(2t/T)^2)\big)}{S_{\nu}(\beta^2)}. \tag{120}$$

For a general α, the term outside the summation requires a power calculation for each value of t.

Dolph-Chebyshev window $\alpha = 0$

The case of $\alpha = 0$ is given by Eq. (56) where the smooth part of the unnormalized window is expressed using the series expansion for $I_1(z)$,

$$I_1(z) = \frac{z}{2} S_1(z^2). \tag{121}$$

Then

$$w(t) = \frac{\beta^2}{2} S_1\big(\beta^2(1-(2t/T)^2)\big) + \frac{T}{2}\delta(|t| - T/2) \qquad -T/2 \leq t \leq T/2 \tag{122}$$

Note that the term $\sqrt{1-(2t/T)^2}$ has been cancelled out. For $\beta = 0$, the window consists of only the delta functions. For $\beta > 0$, the window can be normalized by the value of the smooth part at $t = 0$.

Saramäki window $\alpha = 1$

The formulation in Eq. (118) is particularly efficient for $\alpha = 1$ ($\nu = 0$), since the term in front of the sum evaluates to unity.

$$w(t) = S_0\big(\beta^2(1 - (2t/T)^2)\big), \qquad -T/2 \leq t \leq T/2. \tag{123}$$

This window can be evaluated using only basic arithmetic operations.

Appendix D Setting the End Pulses for Dolph-Chebyshev Windows

In the first section of this appendix, a *discrete-time* Dolph-Chebyshev window is decomposed into two sequences, a bell-shaped sequence and a pulse sequence. It is shown that the pulse sequence can be found from the samples of the bell-shaped sequence along with the value of R, the sidelobe attenuation factor.

While the stopband of a *continuous-time* window is itself equiripple, the sampled window has only an approximately equiripple response. Using the insights gained from the first section, the sampled continuous-time Dolph-Chebyshev window can be tuned to give a better approximation to an equiripple frequency response. This is achieved by controlling the value and/or slope of the frequency response of the sampled window at $\omega = 0$ and $\omega = \pi$. The sampled window can be computed efficiently, avoiding the computational burden of evaluating a discrete-time Chebyshev polynomial.

D.1 Discrete-Time Dolph-Chebyshev Windows

The discrete-time Dolph-Chebyshev windows of §3.3 were decomposed into a bell-shaped sequence and a pulse sequence which is zero except for the end points. In this section, it is shown that the pulse sequence can be uniquely determined using the sidelobe suppression factor R and the middle $N-2$ samples of the window.

Start with an N sample discrete-time Dolph-Chebyshev window. The window is symmetrical: $w[n] = w[N-1-n]$. The interior samples for $n = 1, \ldots, N-2$ outline a bell shape. Append zeros at each end to define the sequence,

$$w_s[n] = \begin{cases} w[n], & n = 1, \ldots, N-2, \\ 0, & \text{elsewhere.} \end{cases} \tag{124}$$

The end points of $w[n]$ have pulses which lie above the immediate neighbours. These end points determine a pulse pair with intermediate zeros,

$$w_p[n] = w[0]\big(\delta[n] + \delta[n-(N-1)]\big). \tag{125}$$

The goal is to determine the value $w[0]$ from $w_s[n]$.

The zero-phase frequency response of an N sample *symmetric* sequence can be written as

$$B_s(\omega) = \sum_{n=0}^{N-1} w_s[n] \cos\big(\omega\big(n - \frac{N-1}{2}\big)\big). \tag{126}$$

The responses at $\omega = 0$ and $\omega = \pi$ are particularly simple to compute

$$
\begin{aligned}
B_s(0) &= \sum_{n=0}^{N-1} w_s[n], \\
B_s(\pi) &= \begin{cases} 0, & N \text{ even}, \\ (-1)^{(N-1)/2} \displaystyle\sum_{n=0}^{N-1} (-1)^n w_s[n], & N \text{ odd}. \end{cases}
\end{aligned}
\tag{127}
$$

The zero-phase frequency response of $w_p[n]$ is

$$
B_p(\omega) = 2\,w[0] \cos\bigl(\frac{\omega}{2}(N-1)\bigr). \tag{128}
$$

At $\omega = 0$ and $\omega = \pi$,

$$
\begin{aligned}
B_p(0) &= 2\,w[0], \\
B_p(\pi) &= \begin{cases} 0, & N \text{ even}, \\ (-1)^{(N-1)/2} B_p(0), & N \text{ odd}. \end{cases}
\end{aligned}
\tag{129}
$$

The cases N odd and N even will be considered separately.

D.1.1 Discrete-time Dolph-Chebyshev window, N odd

For convenience, define $S_N = (-1)^{(N-1)/2}$ which evaluates to ± 1 depending on the parity of $(N-1)/2$. For N odd, the Dolph-Chebyshev window has an extremum at $\omega = \pi$. Since all sidelobe peaks have the same magnitude,

$$
\frac{B_p(0) + B_s(0)}{B_p(\pi) + B_s(\pi)} = S_N R \tag{130}
$$

Then setting $B_p(\pi) = S_N B_p(0)$, for $R > 1$ solve for $B_p(0)$,

$$
B_p(0) = \frac{B_s(0) - S_N B_s(\pi)}{R-1} - S_N B_s(\pi). \tag{131}
$$

This defines the end points of $w[n]$.

With $w[n]$ fully specified, split $w[0] = w_{px}[0] + w_{sx}[0]$, where $w_{px}[n]$ is non-zero for $n = 0$ and $n = N-1$ and will have a sinusoidal frequency response with peak amplitude $B(0)/R$ of the same form as Eq. (128). The sequence $w_{sx}[n]$ is $w_s[n]$ with the end points set.

$$\begin{aligned} 2\,w_{px}[0] &= \frac{B(0)}{R}, \\ 2\,w_{sx}[0] &= B_p(0) - 2\,w_{px}[0]. \end{aligned} \tag{132}$$

The end points of $w_{sx}[n]$ can also be evaluated as

$$2\,w_{sx}[0] = -S_N B_s(\pi). \tag{133}$$

This sets $B_{sx}(\pi) = 0$. The spectrum of $w_{sx}[n]$ will have a double-order zero at $\omega = \pi$.

An example of $w_{sx}[n]$ is shown in Fig. 12 for $N = 33$ and $R = 20$. The thick line in the plot shows $w_{sx}[n]$. All but the end points are samples of a smooth function. The samples of the smooth function have been extrapolated to create two new endpoints (thin lines).[25] The actual end points of $w_{sx}[n]$ are those that set $B_{sx}(\pi) = 0$.

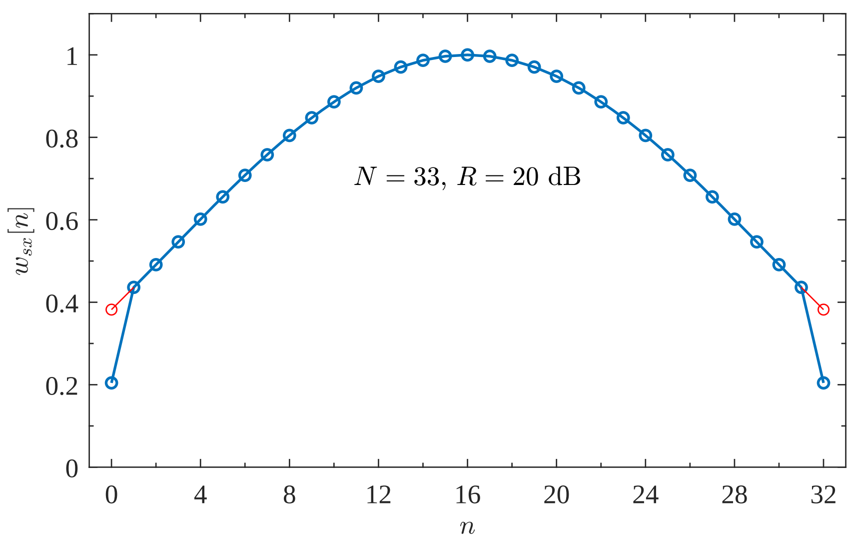

Fig. 12 Plot of $w_{sx}[n]$ (thick line) for a discrete-time Dolph-Chebyshev window. The thin lines show the extensions of the smooth part of the window.

D.1.2 Discrete-time Dolph-Chebyshev window, N even

The discussion above has been for N odd. For N even, $w_p[0]$ will be chosen to control the slope of the spectrum at $\omega = \pi$.

[25]For plotting purposes the endpoints were created by spline extrapolation.

First, some preliminary results.

Slope of $B(\omega)$

The derivative of the Chebyshev polynomial $T_M(x)$ can be shown to be [6, §2.4.5].

$$\frac{d}{dx} T_m(x) = m\, U_{m-1}(x), \tag{134}$$

where $U_m(x)$ ia the Chebyshev polynomial of the second kind and is given in Eq. (9). When $x = x_0 \cos(\omega/2)$,

$$\frac{d}{d\omega} T_m(x_0 \cos(\omega/2)) = -\frac{m}{2} x_0 \sin(\omega/2)\, U_{m-1}\big(x_0 \cos(\omega/2)\big). \tag{135}$$

This is the derivative of a frequency response with peak amplitude R at $\omega = 0$ and sidelobes with peak amplitude one. In the present case, $m = N - 1$ and the frequency response has been scaled by $B(0)/R$. Then the derivative of the zero-phase response of the window is

$$B'(\omega) = -\frac{N-1}{2} \frac{B(0)}{R} x_0 \sin(\omega/2)\, U_{N-2}\big(x_0 \cos(\omega/2)\big). \tag{136}$$

Finally, at $\omega = \pi$ and using the middle line of Eq. (9) to evaluate $U_{N-2}(0)$,[26]

$$B'(\pi) = -\frac{N-1}{2} \frac{B(0)}{R} x_0 \sin\big(\frac{\pi}{2}(N-1)\big). \tag{137}$$

This derivative at $\omega = \pi$ is zero for N odd and non-zero for N even (with alternating signs depending on the parity of $N/2$). For N even,

$$B'(\pi) = D_N x_0 \frac{B(0)}{R}, \qquad N \text{ even}, \tag{138}$$

where for convenience, $D_N = (-1)^{N/2}(N-1)/2$.

Slope of $B_p(\omega)$

Using the zero-phase response of a pair of pulses given by Eq. (128), the derivative is

$$B_p'(\omega) = -B_p(0) \frac{N-1}{2} \sin\big(\frac{\omega}{2}(N-1)\big). \tag{139}$$

[26] Note that x_0 is a function of N and R, see Eq. (27).

The derivative evaluated at $\omega = \pi$ for N even is

$$B_p'(\pi) = D_N B_p(0), \qquad N \text{ even.} \tag{140}$$

Slope of $B_s(\omega)$

The zero-phase response of the samples of the smooth part of the window is given in Eq. (126). The slope is then

$$B_s'(\omega) = -\sum_{n=0}^{N-1} \big(n - \frac{N-1}{2}\big) \sin\big(\omega(n - \frac{N-1}{2})\big) w_s[n]. \tag{141}$$

At $\omega = \pi$ for N even, the slope is

$$B_s'(\pi) = D_N \sum_{n=0}^{N-1} (-1)^n \big(1 - \frac{2n}{N-1}\big) w_s[n], \qquad N \text{ even.} \tag{142}$$

Solving for $B_p(0)$

Equating the slopes at $\omega = \pi$

$$\begin{aligned} B'(\pi) &= B_p'(\pi) + B_s'(\pi) \\ D_N x_0 \frac{B_p(0) + B_s(0)}{R} &= D_N B_p(0) + B_s'(\pi) \end{aligned} \tag{143}$$

Solving for $B_p(0) = 2\,w[0]$,

$$B_p(0) = \frac{B_s(0) - B_s'(\pi)/D_N}{R/x_0 - 1} - B_s'(\pi)/D_N. \tag{144}$$

This defines the end points of $w[n]$. Note that x_0 is expressed as a function of R in Eq. (27) and that for $R > 1$, $R/x_0 > 1$.[27]

With $B(0) = B_p(0) + B_s(0)$ determined, $B_{px}(0)$ can be set,

$$B_{px}(0) = \frac{B(0)}{R}. \tag{145}$$

[27] A degenerate case occurs when $R = 1$ (implies $x_0 = 1$) – the window is all zeros except for the end points.

Then $w_{sx}[n]$ is given by

$$w_{sx}[n] = \begin{cases} \frac{1}{2}\big(B_p(0) - B_{px}(0)\big), & n = 0 \text{ and } n = N-1, \\ w_s[n], & 1 \leq n \leq N-2. \end{cases} \tag{146}$$

Write $B'(\pi)$ and $B'_{px}(\pi)$ as

$$B'(\pi) = D_N x_0 B_{px}(0), \quad B'_{px}(\pi) = D_N B_{px}(0). \tag{147}$$

Then in order to set the slope at $\omega = \pi$ correctly,

$$B'_{sx}(\pi) = D_N(x_0 - 1)B_{px}(0). \tag{148}$$

This requires $w_{sx}[0]$ to cancel out the effect of the middle coefficients $w_s[n]$ and add the term $D_N(x_0 - 1)B_{px}(0)$ to the slope, giving

$$2\,w_{sx}[0] = (x_0 - 1)B_{px}(0) - B'_s(\pi)/D_N. \tag{149}$$

This can be verified algebraically starting from Eq. (146). A plot of $w_{sx}[n]$ for N even has a form similar to that of Fig. 12.

D.2 Sampled Continuous-Time Dolph-Chebyshev Windows

A continuous-time Dolph-Chebyshev window consists of a smooth component plus impulse functions at the end of the window. In §5.2, a first stab at creating an equiripple stopband response was suggested. Here we improve the stopband behaviour by refining the pulses at the end of the window to control the spectrum at both $\omega = 0$ and $\omega = \pi$.

D.2.1 Sampled Continuous-time Dolph-Chebyshev window, N odd

The formalism used to obtain the pulses at the end of the window for discrete-time windows described above will be applied to sampled continuous-time windows. The goal is to have the stopband frequency response $B(\pi)$ equal to the $B(0)/R$. Starting from the $N-2$ middle samples of the sampled window, use the value of R to set the end samples as described in §D.1.1. For the example cited above, this results in a window much closer to having an equiripple stopband.

D.2.2 Sampled Continuous-time Dolph-Chebyshev window, N even

For N even, the goal is set the slope of the frequency response $B'(\pi)$. The procedure described earlier in §D.1.2 uses both R and x_0. The value for x_0 is typically just above one – for a given R, the value of x_0 gets closer to one as N increases. The value of x_0 for a discrete-time window is a function of R and N, see Eq. (27). The value of R for the CT window is given by Eq. (47). Combining these, an estimate for x_0 is

$$x_0 = \cosh\Bigl(\frac{\beta}{N-1}\Bigr). \tag{150}$$

Experiments show that for many cases of practical interest, the estimation of x_0 is not necessary. Using the value $x_0 = 1$ gives good results.

References

[1] A. V. Oppenheim, R. W. Schafer, *Discrete-Time Signal Processing*, 3rd ed., Prentice-Hall, 2010 (ISBN: 978-0-13-198842-2).

[2] P. Kabal, *Time Windows for Linear Prediction of Speech*, Technical Report, Electrical & Computer Engineering, McGill University, Nov. 2009 (on-line at `MMSP.ECE.McGill.CA`).

[3] H. Rohling and J. Schuermann, "Discrete Time Window Functions with Arbitrarily Low Sidelobe Level", *Signal Processing*, vol. 5, no. 2, pp. 127–138, March 1983 (doi: `10.1016/0165-1684(83)90019-1`).

[4] P. Kabal, *Audio File Programs and Routines*, AFsp software package, v10.4a, Sept. 2022 (on-line at `MMSP.ECE.McGill.CA`).

[5] R. L. Streit, "A Two-Parameter Family of Weights for Nonrecursive Digital Filters and Antennas", *IEEE Trans. Acoustics, Speech, Signal Processing*, vol. 32, no. 1, pp. 108–118, Feb. 1984 (doi: `10.1109/TASSP.1984.1164275`).

[6] J. C. Mason and D. C. Handscomb, *Chebyshev Polynomials*, Chapman & Hall, 2003 (ISBN: 978-0-8493-0355-5).

[7] A. G. Deczky, "Unispherical Windows", *IEEE Int. Symp. Circuits, Systems* (Sydney, Australia), pp. II-85–II-88, May 2001 (doi: `10.1109/ISCAS.2001.921012`).

[8] S. W. A. Bergen and A. Antoniou, "Design of Ultraspherical Window Functions with Prescribed Spectral Characteristics", *J. Applied Signal Processing*, vol. 2004, no. 13, pp. 2053–2065, Oct. 2004 (doi: `10.1155/S1110865704403114`).

[9] T. Saramäki, "A Class of Window Functions with Nearly Minimum Sidelobe Energy for Designing FIR Filters", *Proc. IEEE Int. Symp. Circuits, Systems* (Portland, OR), pp. 359–362, May 1989 (doi: `10.1109/ISCAS.1989.100365`).

[10] R. W. Hamming, *Numerical Methods for Scientists and Engineers*, 2nd ed., Dover, 1986 (ISBN: 978-0-486-65241-2).

[11] L. Fox and I. B. Parker, *Chebyshev Polynomials in Numerical Analysis*, Oxford University Press, 1968 (ISBN: 978-0-19859614-1).

[12] P. Kabal, *Real and Complex Finite Length Sequences with Linear Phase Responses*, Technical Report, Electrical & Computer Engineering, McGill University, April 2022 (on-line at `MMSP.ECE.McGill.CA`).

[13] C. L. Dolph, "A Current Distribution for Broadside Arrays Which Optimizes the Relationship Between Beam Width and Side-Lobe Level", *Proc. Inst. Radio Engineers*, vol. 34, no. 6, pp. 335–348, June 1946 (doi: `10.1109/JRPROC.1946.225956`).

[14] G. J. van der Maas, "A Simplified Calculation for Dolph-Tchebycheff Arrays", *J. Applied Physics*, vol. 25, no. 1, pp. 121–124, Jan. 1954 (doi: `10.1063/1.1721495`).

[15] A. Rowińska-Schwarzweller and M. Wintermantel, “On Designing FIR Filters Using Windows Based on Gegenbauer Polynomials”, *Proc. IEEE Int. Symp. Circuits, Systems* (Phoenix-Scottsdale, AZ), pp. I-413–I-416, May 2002 (doi: `10.1109/ISCAS.2002.1009865`)

[16] M. Abramowitz and I. A. Stegun, eds., *Handbook of Mathematical Functions*, Knovel, 1972 (ISBN: 978-0486-61272-0).

[17] T. T. Taylor, *Dolph Arrays of Many Elements*, Technical Memorandum, Hughes Aircraft R&D Lab, document AD0018054, Aug. 1953 (on-line at `apps.dtic.mil/sti/tr/pdf/AD0018054.pdf`).

[18] G. A. Campbell and R. M. Foster, *Fourier Integrals for Practical Applications*, D. Van Nostrand Company, 1948 (ISBN: 978-044201451-3).

[19] J. F. Kaiser and R. W. Schafer, “On the Use of the I_0-sinh Window for Spectrum Analysis”, *IEEE Trans. Acoust., Speech, Signal Processing*, vol. 28, no. 1, pp. 105–107, Feb. 1980 (doi: `10.1109/TASSP.1980.1163349`).

[20] P. Kabal, *Frequency Domain Representations of Sampled and Wrapped Signals*, Technical Report, Electrical & Computer Engineering, McGill University, June 2021. (on-line at `MMSP.ECE.McGill.CA`).

[21] IEEE Signal Processing Committee (eds.), *Programs for Digital Signal Processing*, IEEE Press, 1979 (ISBN: 978-0-471-05962-2).